Distributed Localization of Target for MIMO Radar With Widely Separated Directional Transmitters and Omnidirectional Receivers

KUI XIONG, Student Member, IEEE
GUOLONG CUI, Senior Member, IEEE
WEI YI, Senior Member, IEEE
University of Electronic Science and Technology of China, Chengdu, China

SHIYUAN WANG, Senior Member, IEEE
Southwest University, Chongqing, China

LINGJIANG KONG, Senior Member, IEEE
University of Electronic Science and Technology of China, Chengdu, China

Conventional target localization algorithms for the multiple-input multiple-output (MIMO) radar with widely separated antennas are mainly based on the centralized localization framework, which suffer from huge burdens of computation and communication as well as robustness defect in complex environments. To overcome these issues, this article first considers the MIMO radar with widely separated directional transmitters and omnidirectional receivers generating the bistatic range (BR) and angle of incidence (AOI) measurements for target localization, which is proven that the position of the target can be uniquely determined with one transmitter and one receiver. Then, the distributed localization framework using the hybrid BR and AOI measurements is developed, where each receiver acts as a fusion center extracting the BR and AOI measurements to perform the localization process, and the localization problem is formulated as solving a linear matrix equation. The *distributed constrained total least squares* (DCTLS) algorithm considering errors in both data matrix and observation vector is proposed for each receiver for target localization. The localization performance regarding the Cramér–Rao lower bound is derived for theoretical analysis. Numerical simulations are performed to validate the efficacy and superiority of the proposed DCTLS algorithm over other typical localization algorithms.

Manuscript received 13 June 2022; revised 18 September 2022; accepted 7 November 2022. Date of publication 17 November 2022; date of current version 9 June 2023.

DOI. No. 10.1109/TAES.2022.3221686

Refereeing of this contribution was handled by K. V. Mishra.

This work was supported in part by the National Natural Science Foundation of China under Grant U19B2017, Grant 62271126, Grant 62101097, and Grant 61871080, in part by the ChangJiang Scholar Program, in part by the 111 under Grant B17008, and in part by the China Postdoctoral Science Foundation under Grant 2020M680147 and Grant 2021T140096.

Authors' addresses: Kui Xiong, Guolong Cui, Wei Yi, and Lingjiang Kong are with the School of Information and Communication Engineering, University of Electronic Science and Technology of China, Chengdu 611731, China, E-mail: (kxiong@std.uestc.edu.cn; cuiguolong@uestc.edu.cn; kussoyi@gmail.com; ljkong@uestc.edu.cn); Shiyuan Wang is with the College of Electronic and Information Engineering, Southwest University, Chongqing 400715, China, E-mail: (wsy@swu.edu.cn). *(Corresponding author: Guolong Cui.)*

I. INTRODUCTION

The multiple-input multiple-output (MIMO) radar with widely separated antennas has received considerable attention in recent years thanks to its spatial diversity and high performance [1]. Unless otherwise specified, this type of the MIMO radar, other than the MIMO radar with colocated antennas [2], is only considered in this article. Target localization is of critical importance for the application of the MIMO radar, which can be categorized into direct methods [3], [4], [5], [6] and indirect methods [7], [8], [9], [10], [11], [12]. In the former, the target position is estimated directly by processing the received signals [3], [4], [5], [6]. But in the latter, some measurements are first extracted and collected from observations and then are used to obtain the estimate of the target position [7], [8], [9], [10], [11], [12]. Generally, the direct methods can provide better performance in low signal-to-noise ratio (SNR) scenarios but higher computational and communication burdens than the indirect methods. In addition, the indirect methods can provide closed-form solutions, while the direct methods can only provide asymptotically optimal solutions. Therefore, this article mainly focuses on the indirect method.

The time-dependent measurements including the time of arrival (TOA) and the time difference of arrival (TDOA) are commonly used in the indirect methods due to their decent performance and simplicity of the system. Using these measurements, the localization task is to solve elliptical or hyperbolic equations based on some optimization algorithms. Actually, both TOA and TDOA measurements can be uniformly classified as the bistatic range (BR) measurements of the MIMO radar, and various BR localization algorithms have been presented in recent years. Specifically, the first-order approximation of nonlinear equations is presented in [3] to obtain the best linear unbiased estimator, and some other iterative algorithms [13], [14] are also presented for target localization, but all these methods require an initialization sufficiently close to the actual target position. The closed-form methods are therefore presented to address this problem, which mainly employ various forms of least squares (LS) methods, such as one-stage LS [15], two-stage weighted LS (WLS) [16], [17], [18], one-stage WLS [19], [20], [21], and constrained WLS [22]. In addition, for moving target localization, the Doppler shift (DS) measurement is used with the BR measurement to estimate the target position by presenting various algorithms [9], [10], [11], [23], [24], [25], [26], [27].

When the angle of arrival (AOA) measurements are available for receivers, the improved localization performance can be further achieved by the hybrid BR and AOA algorithm. By applying the compressive sensing technique, the sparsity-aware hybrid TDOA and AOA localization algorithm is presented to obtain a maximum likelihood (ML) estimate of the target position [28], but this algorithm mainly considers the two-dimensional (2-D) localization problem and cannot provide a closed-form solution. Then, two hybrid BR and AOA localization algorithms based on the WLS method are presented [29], [30] to obtain a closed-form solution and better localization performance than the BR only algorithm for the 3-D localization scenario. In addition, a semi closed-form hybrid BR and AOA localization algorithm is presented [31] to solve a convex optimization problem based on an approximately equivalent ML estimation problem. For moving target localization, the hybrid BR, AOA, and DS localization algorithms are also presented [32], [33].

Generally, compared with the BR only algorithms, the hybrid BR and AOA algorithms with a more complex system equipment can provide the improved localization performance, where each receiver needs to be equipped with array antennas to extract the AOA measurements. Despite their respective advantages for target localization, however, two pivotal issues remain unresolved by these two types of algorithms. First of all, these algorithms are presented based on a centralized system architecture, where a fusion center is used to receive measurements from all receivers to obtain an estimate of the target position centrally. Therefore, these algorithms suffer from high computational and communication costs, and would lose their effectiveness when the centralized fusion center is compromised in some electronic countermeasure scenarios. In addition, in many practical applications, the receivers are not capable for equipping with expensive array antennas. For example, all receivers are placed on the unmanned aerial vehicles (UAVs), and the hybrid BR and AOA algorithms are no longer applicable in such a circumstance since the AOA measurements cannot be available. Although the BR only algorithms can be applicable in this case, the localization performance cannot be guaranteed.

For the first issue, various distributed localization algorithms have been presented for wireless sensor networks (WSNs) [34], [35], [36], [37], [38], [39] in past decades. The sensor nodes in the WSN complete the target localization task through local communications and consensus of the whole network owing to their limited resources and capabilities. But the target localization task for the MIMO radar is executed by transmitters and receivers cooperatively, where the radiation range of all transmitters covers the entire surveillance area, and all receivers can receive the reflected target echoes illuminated by all transmitters. This difference means that the localization methods for WSNs cannot be directly adopted in the MIMO radar but some important principles can be used as inspiration to devise the localization method. For the second issue, the MIMO radar with directional transmitters and omnidirectional receivers can be a desirable candidate, in which the transmitters can synthesize directional beams to illuminate the target and transmit the information of the angle of incidence (AOI) regarding transmitters to receivers through communication links, while the receivers can extract the BR and AOI measurements for target localization. Thus, the distributed network architecture for lightweight receivers is required owing to the limited resources of receivers. However, the distributed localization method has not been presented for the MIMO radar and the AOI information has not been utilized for the WSN for target localization until now.

The novel and important results can be obtained by exploiting both advantages of the WSN and the MIMO radar. To this end, this article aims at devising the distributed localization algorithm for the MIMO radar with no centralized fusion center to improve the efficacy and performance of the conventional localization algorithms. The main contributions are summarized as follows.

1) *The MIMO radar system with widely separated directional transmitters and omnidirectional receivers is developed for target localization:* In the formulated MIMO radar system, each transmitter synthesizes a probing beam to scan the surveillance area in azimuth and elevation, while transmitting a communication beam toward receivers to transmit the information of the probing beam to extract the BR and AOI measurements cooperatively. All receivers constitute a distributed network with no centralized fusion center, and each receiver in the network shares the information with its neighbors for target localization. The formulated MIMO radar system bears the potential advantages of antijamming, system robustness, and high localization performance.

2) *The distributed localization framework of the MIMO radar using the hybrid BR and AOI measurements is developed:* First, it is proven that the target position can be uniquely determined using a pair of the BR, azimuth, and elevation. Then, by transforming the equations of the BR, azimuth, and elevation into a linear matrix equation, each receiver uses the BR and AOI measurements to estimate the target position by solving this linear matrix equation individually, and then broadcasts the estimate result to its neighbors. Finally, each receiver receives the estimate results shared by its neighbors and performs the process of estimate combination for accuracy improvement.

3) *The distributed constrained total least squares (DCTLS) localization algorithm is proposed for each receiver of the MIMO radar:* By considering the errors in both the data matrix and the observation vector, a CTLS problem is formulated for solving the linear matrix equation, which is proven to be a unconstrained WLS problem. Thus, the local localization algorithm based on the WLS method is proposed to obtain the local estimate of the target position for each receiver. Then, the estimation covariance for the local estimate is derived, which represents the estimate confidence to generate the weighting coefficient to combine estimate results transmitted from neighbors. Furthermore, the performance analysis of the DCTLS algorithm in terms of the Cramér–Rao lower bound (CRLB) is performed,

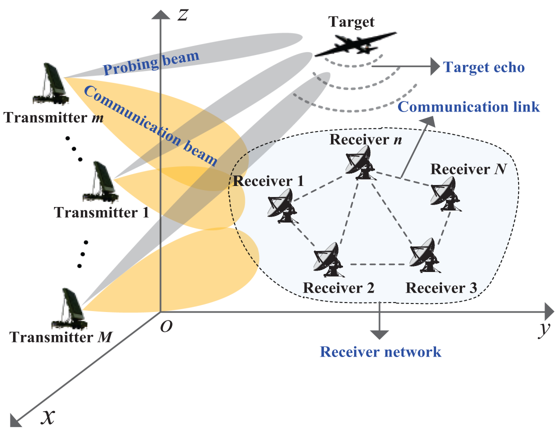

Fig. 1. System model of MIMO radar with directional transmitters and omnidirectional receivers for target localization.

which is proven and validated to be superior to that of the conventional localization algorithms.

The rest of this article is organized as follows. In Section II, the system model of the MIMO radar with directional transmitters and omnidirectional receivers for target localization is developed, then the distributed localization framework is formulated. In Section III, the DCTLS algorithm for target localization is proposed. Section IV provides some numerical simulations to validate the effectiveness of the proposed algorithm. Finally, Section V concludes this article.

II. SYSTEM MODEL AND LOCALIZATION FRAMEWORK

In this section, the system model of the MIMO radar with directional transmitters and omnidirectional receivers for target localization is first developed. Then, the distributed localization framework for receivers of the MIMO radar is formulated with local localization and estimate combination. Furthermore, the target measurement model based on the developed radar system is introduced.

A. System Model

The MIMO radar with widely separated directional transmitters and omnidirectional receivers is considered for target localization, where all transmitters and receivers work with a time synchronization way. As depicted in Fig. 1, each transmitter as a spatially fixed phased array radar synthesizes a probing beam to scan the surveillance area, while transmitting a wide communication beam covering all receivers to transmit the information of the probing signal. Each receiver is also spatially fixed in a processing interval and equipped with an omnidirectional antenna such that the angle measurement cannot be available. Through wireless communications, all receivers constitute a distributed network owing to their limited resources, and there is no centralized fusion center in the network. A target at the unknown position that is assumed to be spatially fixed in a processing interval of the radar needs to be localized by all transmitters and receivers cooperatively.

The 3-D localization problem is considered in this work. Denote the known position of transmitter m ($m = 1, 2, \ldots, M$) as $\mathbf{t}_m = [x_{T,m}, y_{T,m}, z_{T,m}]^{\mathrm{T}}$, the known position of receiver n ($n = 1, 2, \ldots, N$) as $\mathbf{r}_n = [x_{R,n}, y_{R,n}, z_{R,n}]^{\mathrm{T}}$,[1] and the unknown target position to be estimated as $\mathbf{x} = [x, y, z]^{\mathrm{T}}$, where M is the number of transmitters, N is the number of receivers, and $(\cdot)^{\mathrm{T}}$ denotes the transpose of a matrix or a vector.

For the indirect localization method, some measurements of the target need to be used. The well-known TDOA between the channel of the communication and the channel of the target regarding transmitter m and receiver n is given by $\tau_{m,n}$. Since the positions of transmitter m and receiver n are known, the sum of the range between transmitter m and the target and the range between the target and receiver n, i.e., the BR of transmitter m and receiver n regarding the target, can be calculated using $\tau_{m,n}$ as follows:

$$\begin{aligned} d_{m,n} &= \|\mathbf{t}_m - \mathbf{r}_n\| + c\tau_{m,n} \\ &= \|\mathbf{x} - \mathbf{t}_m\| + \|\mathbf{x} - \mathbf{r}_n\| \\ &= d_{T,m} + d_{R,n} \end{aligned} \tag{1}$$

where c is the speed of propagation, $d_{T,m} = \|\mathbf{x} - \mathbf{t}_m\|$ is the range between transmitter m and the target, $d_{R,n} = \|\mathbf{x} - \mathbf{r}_n\|$ is the range between the target and receiver n, and $\|\cdot\|$ denotes the Euclidean norm.

For the formulated MIMO radar with directional transmitters and omnidirectional receivers, the azimuth and elevation of the target corresponding to each transmitter can also be obtained for target localization. The azimuth and elevation of the target corresponding to transmitter m are, respectively, defined by[2]

$$\phi_m = \arctan\left(\frac{y - y_{T,m}}{x - x_{T,m}}\right) \tag{2}$$

$$\theta_m = \arctan\left(\frac{z - z_{T,m}}{(x - x_{T,m})\cos\phi_m + (y - y_{T,m})\sin\phi_m}\right). \tag{3}$$

Conventional MIMO radar systems for target localization are mainly based on the centralized architecture of receivers, where a centralized fusion center is used to collect target measurements from all receivers to estimate the target position. Compared with the conventional radar systems, the formulated MIMO radar with directional transmitters and omnidirectional receivers bears the following three advantages.

1) *Resistance to Mainlobe Jamming Toward Transmitter:* The popular smart jammer is to intercept the radar transmission signal and repost it toward the transmitter after replication and modulation. This directional jamming beam cannot be received by the considered radar system since the

[1] In practical applications, the positions of transmitters and receivers are obtained by some self-localization methods.

[2] The specific process of obtaining the azimuth and elevation of the target from the transmitter is provided in Section II-C.

transmitters do not perform receiving task and the receivers are spatially separated from the transmitters.

2) *Robustness to Single-Point Failure:* Conventional radar systems with centralized architecture suffer from the issue of single-point failure when the centralized fusion center fails to work. But the considered radar system can immune to single-point failure since there is no centralized fusion center for target localization.

3) *Localization With High Accuracy:* All transmitters and receivers can extract the transmitting angular measurements regarding the target through communication beams cooperatively. These measurements can be utilized to update the estimate of the target position for localization accuracy improvement.

Two potential applications of this system model are introduced here. The first application is the cooperative target localization of communication base stations (BSs) (e.g., 5G BSs) and WSNs, where the BS represents a transmitter to transmit beams toward the target and the WSN at the same time, and each sensor in the WSN represents a receiver to extract some measurements together with BSs to estimate the target position. Another application is the cooperative target localization of the hybrid active–passive multistatic radars, where the active transmitters equipped with array antennas transmit beams toward the target and passive receivers, but do not perform receiving and processing tasks, since the echoes toward transmitters are generally contaminated by severe mainlobe jamming.

B. Distributed Localization Framework

Almost all target localization algorithms for the MIMO radar are commonly based on the centralized methods [3], [4], [5], [6], [7], [8], [9], [10], [11], [12], [13], [14], [15], [16], [17], [18], [19], [20], [21], [22], [23], [24], [25], [26], [27], [28], [29], [30], [31], [32], [33], in which a centralized fusion center receives the measurements transmitted from all receivers and then estimates the target position by using all measurements. Generally, the centralized methods can generate an accurate localization result but result in some deficiencies. First, the centralized methods suffer from considerably high complexities of computation and communication between receivers, since all measurements of receivers need to be transmitted to the fusion center to estimate the target position. In addition, the centralized methods lose some degrees of freedom for receivers. Each receiver in the centralized methods can only obtain the measurements of the target but cannot obtain the target position individually. Furthermore, the robustness of the centralized methods cannot be guaranteed in some situations. For example, the centralized methods fail positioning at all when the fusion center is destroyed in some adversarial applications.

To this end, it is necessary to develop a new target localization method to replace the conventional centralized localization methods for practical applications. We start by presenting an important proposition.

PROPOSITION 1 The target position $\mathbf{x} = [x, y, z]^{\mathrm{T}}$ can be uniquely determined by using a pair of exactly known BR $d_{m,n}$, azimuth ϕ_m, and elevation θ_m.

PROOF See Appendix 1. ∎

REMARK 1 Proposition 1 indicates that the target position can be uniquely determined using a pair of exact BR, azimuth, and elevation. Thus, it is theoretically feasible to locate the target by using the BR, azimuth, and elevation measurements with one transmitter and one receiver. This opens up the possibility of the distributed localization, where each receiver can estimate the target position independently and perform the estimate combination for performance improvement after receiving the estimate results from other receivers.

According to Proposition 1, one can have that each receiver using exactly known BR, azimuth, and elevation can obtain the target position, which provides the potential to target localization for receivers of the MIMO radar with the distributed network architecture. Thus, this article develops the distributed localization framework for receivers of the MIMO radar, and the topology of all receivers considered in this work is depicted in Fig. 2(a), where each node represents a receiver, the line between two nodes (i.e., edge) represents that the two receivers can exchange their own estimate results each other. Two extreme cases of Fig. 2(a) are shown in Fig. 2(b) and (c), where Fig. 2(b) shows that each receiver connects with all other receivers and Fig. 2(c) shows that each receiver connects with no other receivers, respectively. The nodes connected to one receiver are called the neighbors of this receiver. All receivers are denoted by a set $\mathcal{R} = \{1, 2, \ldots, N\}$, and receiver n together with its neighbors are collectively denoted by a set $\mathcal{R}_n = \{n\} \cup \mathcal{N}_n$, where $\mathcal{N}_n = \{r_{n,1}, r_{n,2}, \ldots, r_{n,N_n}\}$ with $r_{n,i} \in \mathcal{R}\backslash\{n\}$ and $i = 1, 2, \ldots, N_n$, is the set of neighbors of receiver n, N_n is the number of neighbors of receiver n, and $\mathcal{A}\backslash\mathcal{B}$ indicates that set $\mathcal{B}$ is excluded from set $\mathcal{A}$. The task of each receiver in the MIMO radar is to estimate the target position by using its own measurements and then fuse the estimate results shared by its neighbors. Thus, the target localization process of any receiver $n \in \mathcal{R}$ of the MIMO radar is first to estimate the target position by using its own measurements, and then broadcast the obtained localization result to its neighbors $\mathcal{N}_n$. Receiver n also receives the local localization results shared by its neighbors to obtain the final localization result by combining all localization results for further accuracy improvement. The distributed localization framework for any receiver $n \in \mathcal{R}$ of the MIMO radar is depicted in Fig. 3, where the target localization process includes two steps, namely local localization and estimate combination.

REMARK 2 In addition to bearing the advantages of the traditional MIMO radar system [1], the MIMO radar considered in this work also bears the following two aspects of advantages. That is, the transmitting angular measurements can be used to improve the target localization performance, and the distributed network architecture of receivers with no centralized fusion center can immune to single-point

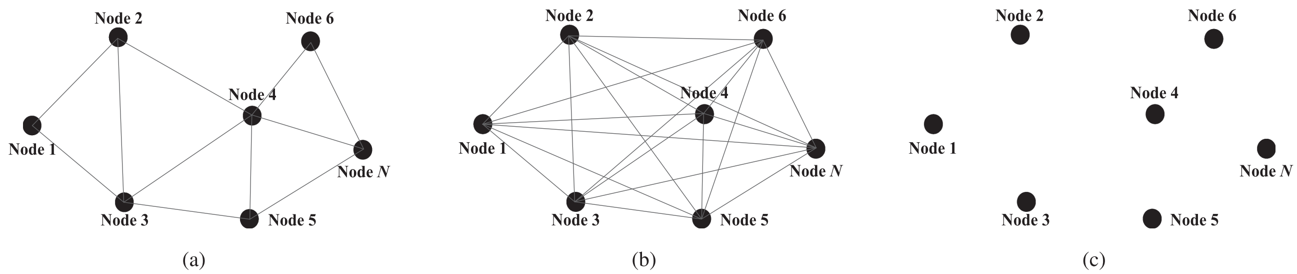

Fig. 2. Topology of receivers with different connectivity: (a) partial connectivity; (b) complete connectivity; (c) no connectivity.

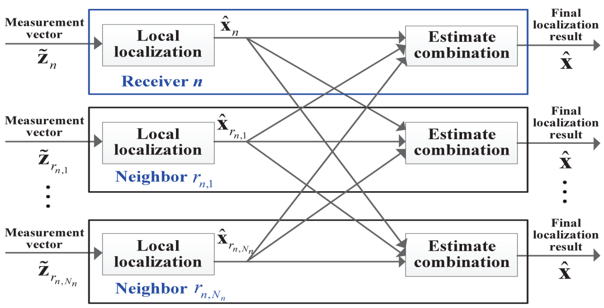

Fig. 3. Distributed localization framework for any receiver n of MIMO radar.

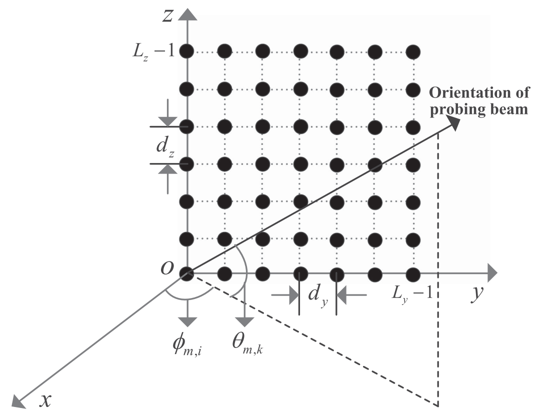

Fig. 4. Deployment of antenna array of transmitter m.

failure. To the best authors' knowledge, the distributed localization framework of the MIMO radar utilizing these two advantages has rarely been explored in the open literature.

C. Measurement Model

Although the indirect localization method is mainly considered in this article, it is necessary to provide the process of obtaining the transmitting angular measurements since this is the first time that the concept and framework of the MIMO radar using this type of measurements for target localization is proposed. When the transmitter has both transmitting and receiving functions, it is common to obtain the azimuth and elevation of the target corresponding to the transmitter by the direction of arrival (DOA) estimation methods [40], [41]. In the sequel, we mainly consider that the transmitter does not have the receiving function, in which each transmitter cooperates with each receiver to obtain the azimuth and elevation of the target.

Actually, transmitter m does not know the azimuth ϕ_m and elevation θ_m of the target in advance, and it synthesizes beams to scan the surveillance area in azimuth and elevation with a predefined order. The orchestration of scanning beams and parameters of the transmission signal are transmitted directly to receiver n through a communication link. Receiver n receives these signals and then performs some processing steps to obtain ϕ_m and θ_m. As a paradigm, assuming that transmitter m is a uniform rectangular planar array consisting of L_y antennas in the y-axis orientation and L_z antennas in the z-axis orientation on the yOz plane, which is depicted in Fig. 4, where d_y and d_z are the interelement spacing in y-axis and z-axis orientations, $\phi_{m,i}$ $(i = 1, 2, \dots, I)$ and $\theta_{m,k}$ $(k = 1, 2, \dots, K)$ are the ith azimuth and kth elevation of the probing beam, and I and K are the number of beams scanning in azimuth and elevation, respectively.

The transmission waveform of all antennas of transmitter m is a narrowband signal $s_m(t)$, and the synthesized probing beam of transmitter m toward azimuth $\phi_{m,i}$ and elevation $\theta_{m,k}$ at central frequency $f_{c,m}$ is therefore given by

$$x_m^{i,k}(t) = \sum_{l_z=0}^{L_z-1}\sum_{l_y=0}^{L_y-1} s_m(t)\exp\left(-j\frac{2\pi}{\lambda_m}(l_y d_y \sin\phi_{m,i}\cos\theta_{m,k} + l_z d_z \sin\theta_{m,k})\right)\exp(j2\pi f_{c,m}t) \quad (4)$$

where $j = \sqrt{-1}$ and λ_m is the wavelength of transmitted signal. And the transmitted communication beam of transmitter m toward receiver n at central frequency $f_{c,m}$ is given by[3]

$$x_m(t) = s_m(t)\exp(j2\pi f_{c,m}t). \quad (5)$$

In practical applications, the transmission signals of any two transmitters m and m' need to satisfy the orthogonal condition, i.e., $\int s_m(t)s^*_{m'}(t)d_t = 0$, where $(\cdot)^*$ denotes the conjugate of a complex-valued signal, or have different carrier frequencies.

[3]The directionality of the communication beam is omitted here for simplicity.

When there is no target in the direction of the transmitted probing beam, the received signal at receiver n is given by

$$y_{m,n}^{i,k}(t) = \alpha_{m,n} x_m(t - t_{c,m,n}) + w_n(t) \tag{6}$$

where $\alpha_{m,n}$ is the communication channel gain, $w_n(t)$ is the zero-mean Gaussian white noise, and $t_{c,m,n}$ is the time delay for communication signal from transmitter m to receiver n, which is given by

$$t_{c,m,n} = \frac{1}{c} \left\| \mathbf{t}_m - \mathbf{r}_n \right\|. \tag{7}$$

When the target located at position $\mathbf{x}$, azimuth $\phi_{m,i_{tar}}$, and elevation $\theta_{m,k_{tar}}$ is illuminated by the transmitted probing beam, the received signal at receiver n is given by

$$y_{m,n}^{i,k}(t) = \alpha_{m,n} x_m(t - t_{c,m,n}) + \beta_{m,n} x_m^{i,k}(t - t_{m,n}) + w_n(t) \tag{8}$$

where $\beta_{m,n}$ is the reflection coefficient for the target, and $t_{m,n}$ is the time delay of the probing signal from transmitter m to the target and then to receiver n, which is given by

$$t_{m,n} = \frac{1}{c}(\|\mathbf{x} - \mathbf{t}_m\| + \|\mathbf{x} - \mathbf{r}_n\|). \tag{9}$$

The differences between the azimuth and elevation of the transmitted probing beam and those of the target are sufficiently small since the angle of the transmitted probing beam is generally small (only a few degrees), i.e., $\phi_{m,i_{tar}} \approx \phi_{m,i}$ and $\theta_{m,k_{tar}} \approx \theta_{m,k}$. Thus, $y_{m,n}^{i,k}(t)$ in (8) can be approximated by

$$\begin{aligned} y_{m,n}^{i,k}(t) &\approx \alpha_{m,n} x_m(t - t_{c,m,n}) \\ &\quad + \beta_{m,n} L_y L_z s_m(t - t_{m,n}) \exp(j2\pi f_{c,m}(t - t_{m,n})) \\ &\quad + w_n(t). \end{aligned} \tag{10}$$

After downconversion, the received baseband signal can be written as

$$z_{m,n}^{i,k}(t) = y_{m,n}^{i,k}(t) \exp(-j2\pi f_{c,m} t). \tag{11}$$

Baseband signal $z_{m,n}^{i,k}(t)$ is then sampled as follows:

$$z_{m,n}^{i,k}(s) = y_{m,n}^{i,k}(s\Delta T) \exp(-j2\pi f_{c,m} s\Delta T) \tag{12}$$

where $s = 1, 2, \ldots, S$ is the fast-time sampling index called the snapshot, S is the number of samples during the dwell time of the transmitted probing beam at an azimuth and elevation, and ΔT is the sampling interval.

Then, receiver n performs the matched filtering process, and the filtering output is given by

$$r_{m,n}^{i,k}(s) = z_{m,n}^{i,k}(s) * s_m^*(-s) \tag{13}$$

where $*$ denotes the convolution operator.

Thus, by detecting IK matched filtering results of $\{r_{m,n}^{i,k}(s)\}_{i,k=1}^{I,K}$, receiver n can obtain the indexes of the probing beam in azimuth and elevation that exhibit the two significant amplitude characteristics (one for communication time delay and another for target echo time delay), i.e., i_{tar} and k_{tar}. Then, the azimuth and elevation at which the target is located are therefore obtained as $\phi_m \approx \phi_{m,i_{\text{tar}}}$ and $\theta_m \approx \theta_{m,k_{\text{tar}}}$, respectively. In addition, the TDOA can also be obtained as $\tau_{m,n} \approx t_{m,n} - t_{c,m,n}$. The conceptual description of above processes for obtaining azimuth ϕ_m and elevation θ_m is depicted in Fig. 5 specifically.

The TDOA $\tau_{m,n}$ (equivalent to BR $d_{m,n}$), azimuth ϕ_m, and elevation θ_m obtained above are not accurate owing to system noises and some physical factors. The actual azimuth and elevation at which the target is located inevitably deviate from the central axis of the probing beam. Generally, the BR is estimated by some parameter estimation methods based on the signal model $r_{m,n}^{i,k}(t)$, such as the ML estimation method [42], but the estimation error is inevitably generated owing to the existence of noises. Thus, the measurements of $d_{m,n}$, ϕ_m, and θ_m are represented as follows:

$$\tilde{d}_{m,n} = d_{m,n} + n_{d,m,n} \tag{14}$$

$$\tilde{\phi}_{m,n} = \phi_m + n_{\phi,m,n} \tag{15}$$

$$\tilde{\theta}_{m,n} = \theta_m + n_{\theta,m,n} \tag{16}$$

where $n_{d,m,n}$, $n_{\phi,m,n}$, and $n_{\theta,m,n}$ are measurement errors of $d_{m,n}$, ϕ_m, and θ_m, respectively, which are assumed to be independent identified distributed (i.i.d.) zero-mean Gaussian variables with variances of $\sigma_{d,m,n}^2$, $\sigma_{\phi,m,n}^2$, and $\sigma_{\theta,m,n}^2$. Here, the subscript n is introduced in $\tilde{\phi}_{m,n}$ and $\tilde{\theta}_{m,n}$ because the measurement errors $n_{\phi,m,n}$ and $n_{\theta,m,n}$ are not only dependent to the array manifold of transmitter m, but also dependent to the SNR of the channel between transmitter m and receiver n.[4] In addition, $\tilde{\phi}_{m,n}$ and $\tilde{\theta}_{m,n}$ are treated as the actual azimuth and elevation of the transmitting beam, while $\phi_{m,n}$ and $\theta_{m,n}$ are the actual azimuth and elevation of the target. In this work, $\tilde{\phi}_{m,n}$ and $\tilde{\theta}_{m,n}$ are uniformly termed as the AOI measurements.

For each receiver (let receiver n be an example without loss of generality), it can obtain M BR measurements $\tilde{\mathbf{z}}_{d,n} = [\tilde{d}_{1,n}, \tilde{d}_{2,n}, \ldots, \tilde{d}_{M,n}]^{\mathrm{T}}$, M azimuth measurements $\tilde{\mathbf{z}}_{\phi,n} = [\tilde{\phi}_{1,n}, \tilde{\phi}_{2,n}, \ldots, \tilde{\phi}_{M,n}]^{\mathrm{T}}$, and M elevation measurements $\tilde{\mathbf{z}}_{\theta,n} = [\tilde{\theta}_{1,n}, \tilde{\theta}_{2,n}, \ldots, \tilde{\theta}_{M,n}]^{\mathrm{T}}$. The corresponding measurement error vectors of $\tilde{\mathbf{z}}_{d,n}$, $\tilde{\mathbf{z}}_{\phi,n}$, and $\tilde{\mathbf{z}}_{\theta,n}$ are given as $\mathbf{n}_{d,n}$, $\mathbf{n}_{\phi,n}$, and $\mathbf{n}_{\theta,n}$, respectively. Stacking all these measurements yields

$$\tilde{\mathbf{z}}_n = \mathbf{z}_n + \mathbf{n}_n \tag{17}$$

where $\mathbf{z}_n = [\mathbf{z}_{d,n}^{\mathrm{T}}, \mathbf{z}_{\phi,n}^{\mathrm{T}}, \mathbf{z}_{\theta,n}^{\mathrm{T}}]^{\mathrm{T}}$ is the actual measurement vector of receiver n, and $\mathbf{n}_n = [\mathbf{n}_{d,n}^{\mathrm{T}}, \mathbf{n}_{\phi n}^{\mathrm{T}}, \mathbf{n}_{\theta n}^{\mathrm{T}}]^{\mathrm{T}}$ is the corresponding measurement error vector with covariance matrix $\mathbf{Q}_n = \text{blkdiag}\{\mathbf{Q}_{d,n}, \mathbf{Q}_{\phi,n}, \mathbf{Q}_{\theta,n}\}$, here $\mathbf{Q}_{d,n} = \text{diag}\{\sigma_{d,1,n}^2, \sigma_{d,2,n}^2, \ldots, \sigma_{d,M,n}^2\}$, $\mathbf{Q}_{\phi,n} = \text{diag}\{\sigma_{\phi,1,n}^2, \sigma_{\phi,2,n}^2, \ldots, \sigma_{\phi,M,n}^2\}$, and $\mathbf{Q}_{\theta,n} = \text{diag}\{\sigma_{\theta,1,n}^2, \sigma_{\theta,2,n}^2, \ldots, \sigma_{\theta,M,n}^2\}$ are the covariance matrices of the BR, azimuth, and elevation measurement error vectors, respectively. Covariance matrix $\mathbf{Q}_n$ is treated as a known quantity since it can be adopted as the theoretical CRLB matrix for the estimation of measurement vector $\mathbf{z}_n$.

[4]The subscript n of $\tilde{\phi}_{m,n}$ and $\tilde{\theta}_{m,n}$ can be omitted when transmitter m has both transmitting and receiving functions since $\tilde{\phi}_{m,n}$ and $\tilde{\theta}_{m,n}$ are independent to receiver n in such a case.

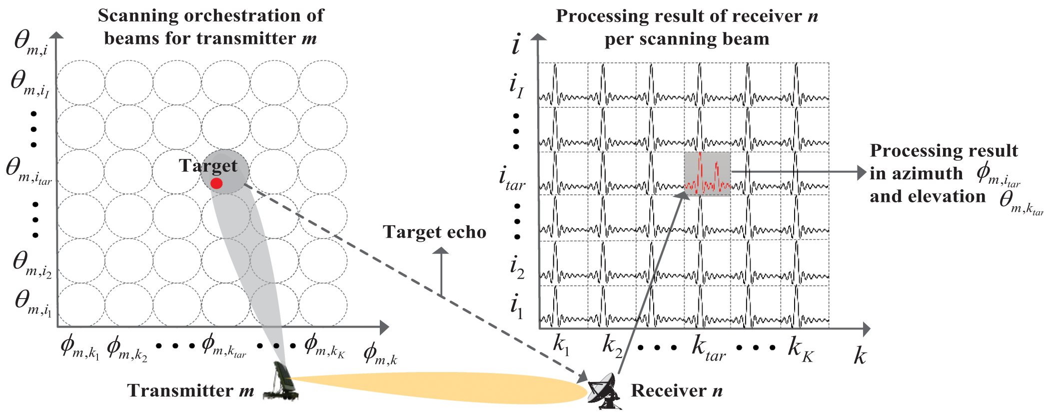

Fig. 5. Scanning orchestration of beams of transmitter m and the corresponding signal processing result of receiver n.

In the developed system model, the BR and AOI measurements are obtained by directional transmitters and omnidirectional receivers cooperatively, but the AOA measurements are extracted by directional receivers in the conventional system model for the hybrid BR and AOA localization [28], [29], [30], [31]. However, the distributed network architecture of receivers is developed here but the centralized one is considered for all conventional localization algorithms for the MIMO radar [3], [4], [5], [6], [7], [8], [9], [10], [11], [12], [13], [14], [15], [16], [17], [18], [19], [20], [21], [22], [23], [24], [25], [26], [27], [28], [29], [30], [31], [32], [33]. Although the network architecture of receivers is similar to that of the WSN [34], [35], [36], [37], [38], [39], the whole system model for transmitters and receivers is different, since all receivers can utilize the AOI measurements for target localization in this work.

III. PROPOSED DISTRIBUTED LOCALIZATION ALGORITHM

In this section, the local localization algorithm based on the CTLS method is first proposed. Then, an estimate combination rule based on the estimation covariance is presented for receivers to fuse the localization results transmitted from other receivers. Finally, the performance analysis of the proposed algorithm is performed.

A. Local Localization

For the developed distributed localization framework for receivers of the MIMO radar, it includes two steps of local localization and estimate combination. It is noteworthy that there is no centralized fusion center in the developed system model, but each receiver acts as a fusion center and can use some localization methods to solve linear matrix (24) to estimate the target position. This process can be named as local localization.

For target localization, the BR, azimuth, and elevation given in (1), (2), and (3) should be transformed to linear forms. First, the BR given in (1) can be rewritten as $d_{m,n} - d_{T,m} = d_{R,n}$, then taking the square of both sides of it yields

$$d_{m,n}^2 + \|\mathbf{t}_m\|^2 - \|\mathbf{r}_n\|^2 = 2(\mathbf{t}_m - \mathbf{r}_n)^{\mathrm{T}}\mathbf{x} + 2d_{m,n}d_{T,m}. \quad (18)$$

In order to obtain a linear equation of the unknown target position $\mathbf{x}$, the range between transmitter m and the target, i.e., $d_{T,m}$, needs to be replaced with an explicit known variable. Using the similar method as in [29], one can obtain

$$\mathbf{x} - \mathbf{t}_m = d_{T,m}\mathbf{u}_{m,n} \quad (19)$$

where $\mathbf{u}_{m,n} = [\cos\phi_{m,n}\cos\theta_{m,n}, \sin\phi_{m,n}\cos\theta_{m,n}, \sin\theta_{m,n}]^{\mathrm{T}}$, and it can be readily observed that $\mathbf{u}_{m,n}^{\mathrm{T}}\mathbf{u}_{m,n} = 1$. Thus, multiplying each term of (18) by $\mathbf{u}_{m,n}^{\mathrm{T}}\mathbf{u}_{m,n}$ yields

$$d_{m,n}^2 + \|\mathbf{t}_m\|^2 - \|\mathbf{r}_n\|^2 = 2(\mathbf{t}_m - \mathbf{r}_n)^{\mathrm{T}}\mathbf{x} + 2d_{m,n}\mathbf{u}_{m,n}^{\mathrm{T}}d_{T,m}\mathbf{u}_{m,n}. \quad (20)$$

Then, substituting (19) into (20) further gives

$$2(d_{m,n}\mathbf{u}_{m,n} + \mathbf{t}_m - \mathbf{r}_n)^{\mathrm{T}}\mathbf{x} = d_{m,n}^2 + \|\mathbf{t}_m\|^2 - \|\mathbf{r}_n\|^2 + 2d_{m,n}\mathbf{u}_{m,n}^{\mathrm{T}}\mathbf{t}_m. \quad (21)$$

Taking the tangent of the azimuth (2) gives

$$\mathbf{v}_{m,n}^{\mathrm{T}}\mathbf{x} = \mathbf{v}_{m,n}^{\mathrm{T}}\mathbf{t}_m \quad (22)$$

where $\mathbf{v}_{m,n} = [\sin\phi_{m,n}, -\cos\phi_{m,n}, 0]^{\mathrm{T}}$. In addition, taking the tangent of the azimuth (3) gives

$$\mathbf{w}_{m,n}^{\mathrm{T}}\mathbf{x} = \mathbf{w}_{m,n}^{\mathrm{T}}\mathbf{t}_m \quad (23)$$

where

$$\mathbf{w}_{m,n} = [\cos\phi_{m,n}\sin\theta_{m,n}, \sin\phi_{m,n}\sin\theta_{m,n}, -\cos\theta_{m,n}]^{\mathrm{T}}.$$

Note that all the three transformations of BR (21), azimuth (22), and elevation (23) are linear equations of the unknown target position $\mathbf{x}$. Replacing actual $d_{m,n}$, $\phi_{m,n}$, and $\theta_{m,n}$ with their measurements $\tilde{d}_{m,n}$, $\tilde{\phi}_{m,n}$, and $\tilde{\theta}_{m,n}$, respectively, and combining all equations give the linear matrix equation of the target position as follows:

$$\tilde{\mathbf{A}}_n\mathbf{x} = \tilde{\mathbf{b}}_n \quad (24)$$

where

$$\tilde{\mathbf{A}}_n = \begin{bmatrix} \tilde{\mathbf{A}}_{u,n} \\ \tilde{\mathbf{A}}_{v,n} \\ \tilde{\mathbf{A}}_{w,n} \end{bmatrix} \quad (25)$$

$$\tilde{\mathbf{A}}_{u,n} = \begin{bmatrix} 2(\tilde{d}_{1,n}\tilde{\mathbf{u}}_{1,n} + \mathbf{t}_1 - \mathbf{r}_n)^{\mathrm{T}} \\ 2(\tilde{d}_{2,n}\tilde{\mathbf{u}}_{2,n} + \mathbf{t}_2 - \mathbf{r}_n)^{\mathrm{T}} \\ \vdots \\ 2(\tilde{d}_{M,n}\tilde{\mathbf{u}}_{M,n} + \mathbf{t}_M - \mathbf{r}_n)^{\mathrm{T}} \end{bmatrix} \tag{25a}$$

$$\tilde{\mathbf{A}}_{v,n} = [\tilde{\mathbf{v}}_{1,n}, \tilde{\mathbf{v}}_{2,n}, \ldots, \tilde{\mathbf{v}}_{M,n}]^{\mathrm{T}} \tag{25b}$$

$$\tilde{\mathbf{A}}_{w,n} = [\tilde{\mathbf{w}}_{1,n}, \tilde{\mathbf{w}}_{2,n}, \ldots, \tilde{\mathbf{w}}_{M,n}]^{\mathrm{T}} \tag{25c}$$

and

$$\tilde{\mathbf{b}}_n = \begin{bmatrix} \tilde{\mathbf{b}}_{u,n} \\ \tilde{\mathbf{b}}_{v,n} \\ \tilde{\mathbf{b}}_{w,n} \end{bmatrix} \tag{26}$$

$$\tilde{\mathbf{b}}_{u,n} = \begin{bmatrix} \tilde{d}_{1,n}^2 + \|\mathbf{t}_1\|^2 - \|\mathbf{r}_n\|^2 + 2\tilde{d}_{1,n}\tilde{\mathbf{u}}_{1,n}^{\mathrm{T}}\mathbf{t}_1 \\ \tilde{d}_{2,n}^2 + \|\mathbf{t}_2\|^2 - \|\mathbf{r}_n\|^2 + 2\tilde{d}_{2,n}\tilde{\mathbf{u}}_{2,n}^{\mathrm{T}}\mathbf{t}_2 \\ \vdots \\ \tilde{d}_{M,n}^2 + \|\mathbf{t}_M\|^2 - \|\mathbf{r}_n\|^2 + 2\tilde{d}_{M,n}\tilde{\mathbf{u}}_{M,n}^{\mathrm{T}}\mathbf{t}_M \end{bmatrix} \tag{26a}$$

$$\tilde{\mathbf{b}}_{v,n} = [\tilde{\mathbf{v}}_{1,n}^{\mathrm{T}}\mathbf{t}_1, \tilde{\mathbf{v}}_{2,n}^{\mathrm{T}}\mathbf{t}_2, \ldots, \tilde{\mathbf{v}}_{M,n}^{\mathrm{T}}\mathbf{t}_M]^{\mathrm{T}} \tag{26b}$$

$$\tilde{\mathbf{b}}_{w,n} = [\tilde{\mathbf{w}}_{1,n}^{\mathrm{T}}\mathbf{t}_1, \tilde{\mathbf{w}}_{2,n}^{\mathrm{T}}\mathbf{t}_2, \ldots, \tilde{\mathbf{w}}_{M,n}^{\mathrm{T}}\mathbf{t}_M]^{\mathrm{T}}. \tag{26c}$$

Note that matrix $\tilde{\mathbf{A}}_n \in \mathbb{R}^{3M\times 3}$ and vector $\tilde{\mathbf{b}}_n \in \mathbb{R}^{3M\times 1}$ can be treated as the data matrix and the observation vector in the linear matrix equation [43], respectively.

When both $\tilde{\mathbf{A}}_n$ and $\tilde{\mathbf{b}}_n$ are known exactly, the exact target position can be derived as $\mathbf{x} = \tilde{\mathbf{A}}_n^{\dagger}\tilde{\mathbf{b}}_n$, where $(\cdot)^{\dagger}$ denotes the Moore–Penrose inverse of a matrix. This is obviously unrealistic because measurement vector $\tilde{\mathbf{z}}_n$ is contaminated by measurement error vector $\mathbf{n}_n$ in practical applications according to (17). The well-known LS method [43] has been presented by considering the error in observation vector $\tilde{\mathbf{b}}_n$, whose estimate result can be obtained as follows:

$$\begin{aligned} \hat{\mathbf{x}} &= \arg\min_{\mathbf{x}} \left\|\tilde{\mathbf{A}}_n\mathbf{x} - \tilde{\mathbf{b}}_n\right\|^2 \\ &= (\tilde{\mathbf{A}}_n^{\mathrm{T}}\tilde{\mathbf{A}}_n)^{-1}\tilde{\mathbf{A}}_n^{\mathrm{T}}\tilde{\mathbf{b}}_n \end{aligned} \tag{27}$$

with $(\cdot)^{-1}$ denoting the inverse of a matrix. However, the localization performance of the LS method cannot be guaranteed since it does not consider the error in data matrix $\tilde{\mathbf{A}}_n$. One can see that both $\tilde{\mathbf{A}}_n$ and $\tilde{\mathbf{b}}_n$ in the considered localization problem are not exactly known owing to the existence of errors in both BR and AOI measurements. To this end, it is necessary to devise a new localization algorithm by considering the errors in both $\tilde{\mathbf{A}}_n$ and $\tilde{\mathbf{b}}_n$.

In the process of local localization, all the measured and received measurements of receiver n can be stacked as $\tilde{\mathbf{z}}_n = \mathbf{z}_n + \mathbf{n}_n$ given in (17), and thus data matrix $\tilde{\mathbf{A}}_n$ and data vector $\tilde{\mathbf{b}}_n$ given in (24) are actually functions of $\tilde{\mathbf{z}}_n$, i.e., $\tilde{\mathbf{A}}_n = \mathbf{A}_n(\tilde{\mathbf{z}}_n)$ and $\tilde{\mathbf{b}}_n = \mathbf{b}_n(\tilde{\mathbf{z}}_n)$. From (17), $\mathbf{z}_n = \tilde{\mathbf{z}}_n - \mathbf{n}_n$ can be readily obtained, and (24) can be rewritten as

$$\mathbf{A}_n(\tilde{\mathbf{z}}_n - \mathbf{n}_n)\mathbf{x} = \mathbf{b}_n(\tilde{\mathbf{z}}_n - \mathbf{n}_n). \tag{28}$$

Note both $\tilde{\mathbf{A}}_n$ and $\tilde{\mathbf{b}}_n$ are contaminated by errors. Thus, taking their Taylor expansions around $\tilde{\mathbf{z}}_n$ and ignoring the second-order and higher-order terms (the specific derivation is provided in Appendix 2) give

$$(\tilde{\mathbf{A}}_n - \Delta\mathbf{A}_n)\mathbf{x} = \tilde{\mathbf{b}}_n - \Delta\mathbf{b}_n \tag{29}$$

where

$$\Delta\mathbf{A}_n = [\mathbf{G}_n^1\mathbf{n}_n, \mathbf{G}_n^2\mathbf{n}_n, \mathbf{G}_n^3\mathbf{n}_n] \tag{30}$$

$$\Delta\mathbf{b}_n = \mathbf{G}_n^4\mathbf{n}_n \tag{31}$$

with $\mathbf{G}_n^1$, $\mathbf{G}_n^2$, $\mathbf{G}_n^3$, and $\mathbf{G}_n^4$ being given in (56), (57), (58), and (60), respectively.

Substituting (30) and (31) into (29) yields

$$\begin{aligned} \tilde{\mathbf{A}}_n\mathbf{x} - \tilde{\mathbf{b}}_n &= \Delta\mathbf{A}_n\mathbf{x} - \Delta\mathbf{b}_n \\ &= x\mathbf{G}_n^1\mathbf{n}_n + y\mathbf{G}_n^2\mathbf{n}_n + z\mathbf{G}_n^3\mathbf{n}_n - \mathbf{G}_n^4\mathbf{n}_n \\ &= \mathbf{G}_n\mathbf{n}_n \end{aligned} \tag{32}$$

where $\mathbf{G}_n = x\mathbf{G}_n^1 + y\mathbf{G}_n^2 + z\mathbf{G}_n^3 - \mathbf{G}_n^4$.

Thus, based on the CTLS method [43], [44], the unknown target position can be estimated by receiver n by solving the following constrained optimization problem:

$$\begin{cases} \min\limits_{\mathbf{x}} \mathbf{n}_n^{\mathrm{T}}\mathbf{Q}_n^{-1}\mathbf{n}_n \\ \text{s.t. } \tilde{\mathbf{A}}_n\mathbf{x} - \tilde{\mathbf{b}}_n = \mathbf{G}_n\mathbf{n}_n \end{cases} \tag{33}$$

where $\mathbf{Q}_n = E[\mathbf{n}_n\mathbf{n}_n^{\mathrm{T}}]$ is the covariance matrix of measurement error vector $\mathbf{n}_n$, and $E[\cdot]$ denotes the mathematical expectation. This constrained optimization problem can be transformed to an unconstrained one by the following proposition.

PROPOSITION 2 The CTLS problem given in (33) is equivalent to the following unconstrained optimization problem:

$$\min_{\mathbf{x}} (\tilde{\mathbf{A}}_n\mathbf{x} - \tilde{\mathbf{b}}_n)^{\mathrm{T}}(\mathbf{G}_n\mathbf{Q}_n\mathbf{G}_n^{\mathrm{T}})^{-1}(\tilde{\mathbf{A}}_n\mathbf{x} - \tilde{\mathbf{b}}_n). \tag{34}$$

PROOF See Appendix 3. ■

REMARK 3 The errors in $\tilde{\mathbf{A}}_n$ and $\tilde{\mathbf{b}}_n$ can be written as an augmented matrix $[\mathbf{E}_n, \mathbf{e}_n]$ whose column vectors are statistically correlated with each other, where $\mathbf{E}_n$ and $\mathbf{e}_n$ are errors in $\tilde{\mathbf{A}}_n$ and $\tilde{\mathbf{b}}_n$, respectively. In the formulated CTLS problem (33), the augmented matrix $[\Delta\mathbf{A}_n, \Delta\mathbf{b}_n]$ with $\Delta\mathbf{A}_n = [\mathbf{G}_n^1\mathbf{n}_n, \mathbf{G}_n^2\mathbf{n}_n, \mathbf{G}_n^3\mathbf{n}_n]$ and $\Delta\mathbf{b}_n = \mathbf{G}_n^4\mathbf{n}_n$ is used to suppress the influence of the error matrix $[\mathbf{E}_n, \mathbf{e}_n]$. The column vectors of $[\Delta\mathbf{A}_n, \Delta\mathbf{b}_n]$ are statistically correlated with each other, because they are all multiplied by the vector $\mathbf{n}_n$. Thus, the problem (33) explores the case where the error components of the data matrix $\tilde{\mathbf{A}}_n$ may be statistically correlated or statistically unrelated but with different variances.

From Proposition 2, one can have that the formulated CTLS problem takes the same form as the WLS problem [16], [17], [18], [19], [20], [21] with weighting matrix $(\mathbf{G}_n\mathbf{Q}_n\mathbf{G}_n^{\mathrm{T}})^{-1}$, and the same methods that solve the WLS problem can also be adopted to solve problem (34). Thus, the target position can be estimated by receiver n by applying the WLS method as follows:

$$\hat{\mathbf{x}}_n = (\tilde{\mathbf{A}}_n^{\mathrm{T}}\mathbf{W}_n\tilde{\mathbf{A}}_n)^{-1}\tilde{\mathbf{A}}_n^{\mathrm{T}}\mathbf{W}_n\tilde{\mathbf{b}}_n \tag{35}$$

where $\mathbf{W}_n = (\mathbf{G}_n\mathbf{Q}_n\mathbf{G}_n^{\mathrm{T}})^{-1}$ is the weighting matrix. Generally, it is difficult to design the weighting matrix for the

WLS algorithm, and various methods have been presented to identify the weighting matrix in the WLS algorithms [16], [17], [18], [19], [20], [21], but the determinate form of the weighting matrix is obtained here thanks to Proposition 2.

Note that weighting matrix $\mathbf{W}_n$ is unknown since it is dependant on the unknown matrix $\mathbf{G}_n$. To implement the WLS method to estimate $\mathbf{x}$, $\mathbf{W}_n = \mathbf{Q}_n^{-1}$ is used for the initial estimate, and then obtains more accurate $\mathbf{W}_n$ according to (35), thus resulting in more accurate estimate of $\mathbf{x}$.

B. Estimate Combination

After completing local localization for the target, each receiver receives the estimate results transmitted from its neighbors and then performs estimate combination. For the estimate result obtained by each receiver, the estimate of the target position and the corresponding estimate accuracy are the two crucial factors. Denote the estimate bias of the target position for receiver n as follows:

$$\begin{aligned}\Delta\mathbf{x}_n &= \mathbf{x} - \hat{\mathbf{x}}_n\\ &= (\tilde{\mathbf{A}}_n^{\mathrm{T}}\mathbf{W}_n\tilde{\mathbf{A}}_n)^{-1}\tilde{\mathbf{A}}_n^{\mathrm{T}}\mathbf{W}_n\tilde{\mathbf{A}}_n\mathbf{x}\\ &\quad - (\tilde{\mathbf{A}}_n^{\mathrm{T}}\mathbf{W}_n\tilde{\mathbf{A}}_n)^{-1}\tilde{\mathbf{A}}_n^{\mathrm{T}}\mathbf{W}_n\tilde{\mathbf{b}}_n\\ &= (\tilde{\mathbf{A}}_n^{\mathrm{T}}\mathbf{W}_n\tilde{\mathbf{A}}_n)^{-1}\tilde{\mathbf{A}}_n^{\mathrm{T}}\mathbf{W}_n\mathbf{e}_n. \end{aligned} \tag{36}$$

Ignoring the second-order and higher-order noise terms in $\Delta\mathbf{x}_n$ and taking mathematical expectation give $E[\hat{\mathbf{x}}_n] \approx \mathbf{x}$. This implies that the local estimator also generates an unbiased estimate. The covariance of the estimate of the target position for receiver n is therefore given by

$$\hat{\mathbf{R}}_n = E[\Delta\mathbf{x}_n(\Delta\mathbf{x}_n)^{\mathrm{T}}] \approx (\mathbf{A}_n^{\mathrm{T}}\mathbf{W}_n\mathbf{A}_n)^{-1} \tag{37}$$

where matrix $\mathbf{A}_n$ is the noise-free version of data matrix $\tilde{\mathbf{A}}_n$. In practice, matrix $\mathbf{A}_n$ is not available, and thus the noisy version $\tilde{\mathbf{A}}_n$ is used to generate $\hat{\mathbf{R}}_n$. Then, the obtained covariance matrix $\hat{\mathbf{R}}_n$ together with the estimate of the target position $\hat{\mathbf{x}}_n$ are transmitted by receiver n to its neighbors to obtain the final combined estimate.

After receiving the estimate results of the target position and the corresponding covariance matrices from all neighbors, receiver n uses the following combination rule to obtain the final estimate of the target position:

$$\hat{\mathbf{x}} = \sum_{i\in\mathcal{R}_n} w_i\hat{\mathbf{x}}_i \tag{38}$$

where w_i is the combination coefficient that satisfies

$$\sum_{i\in\mathcal{R}_n} w_i = 1 \text{ and } w_i \geq 0. \tag{39}$$

In this work, the combination coefficient for receiver $i \in \mathcal{R}_n$ using the covariance matrix of the estimate of the target position is given as follows:

$$w_i = \frac{(\det(\hat{\mathbf{R}}_i))^{-1}}{\sum_{j\in\mathcal{R}_n}(\det(\hat{\mathbf{R}}_j))^{-1}} \tag{40}$$

where $\det(\cdot)$ denotes the determinant of a matrix.

Algorithm 1: Distributed Constrained Total Least Squares Algorithm for Target Localization.

Input: Measurement vector $\tilde{\mathbf{z}}_n$ with covariance $\mathbf{Q}_n$ for any receiver $n \in \mathcal{R}$.

Local Localization: For each receiver $n \in \mathcal{R}$, performing following steps:

1) Generate data matrix $\tilde{\mathbf{A}}_n$ and data vector $\tilde{\mathbf{b}}_n$ using (25) and (26), respectively.
2) Set initial weighting matrix as $\mathbf{W}_n = \mathbf{Q}_n^{-1}$ and initial estimate of target position as
$$\hat{\mathbf{x}}_n = (\tilde{\mathbf{A}}_n^{\mathrm{T}}\mathbf{W}_n\tilde{\mathbf{A}}_n)^{-1}\tilde{\mathbf{A}}_n^{\mathrm{T}}\mathbf{W}_n\tilde{\mathbf{b}}_n.$$
3) Generate matrix $\mathbf{G}_n = \hat{x}_n\mathbf{G}_n^1 + \hat{y}_n\mathbf{G}_n^2 + \hat{z}_n\mathbf{G}_n^3 - \mathbf{G}_n^4$ and update weighting matrix as
$$\mathbf{W}_n = (\mathbf{G}_n\mathbf{Q}_n\mathbf{G}_n^{\mathrm{T}})^{-1}.$$
4) Update estimate of target position as
$$\hat{\mathbf{x}}_n = (\tilde{\mathbf{A}}_n^{\mathrm{T}}\mathbf{W}_n\tilde{\mathbf{A}}_n)^{-1}\tilde{\mathbf{A}}_n^{\mathrm{T}}\mathbf{W}_n\tilde{\mathbf{b}}_n.$$
5) Compute estimation covariance matrix as
$$\hat{\mathbf{R}}_n = (\tilde{\mathbf{A}}_n^{\mathrm{T}}\mathbf{W}_n\tilde{\mathbf{A}}_n)^{-1}.$$

Estimate Combination: After receiving estimation results from its neighbors $\mathcal{R}_n$, performing following steps:

1) Compute combination weight w_i for each receiver as
$$w_i = \frac{(\det(\hat{\mathbf{R}}_i))^{-1}}{\sum_{j\in\mathcal{R}_n}(\det(\hat{\mathbf{R}}_j))^{-1}}.$$
2) Compute combined estimate as
$$\hat{\mathbf{x}} = \sum_{i\in\mathcal{R}_n} w_i\hat{\mathbf{x}}_i.$$

Output: Estimated target position $\hat{\mathbf{x}}$ for receiver n.

So far, all the derivations of the distributed localization algorithm have been completed, which is named the DCTLS algorithm and is summarized in Algorithm 1 specifically.

REMARK 4 Three differences of the proposed DCTLS algorithm compared with the conventional algorithms [28], [29], [30], [31] can be highlighted as follows. First, the different distributed network architecture of receivers is developed for the DCTLS algorithm, which is the first exploration in the MIMO radar for target localization. In addition, the hybrid BR and AOI measurements are used in the DCTLS algorithm, and the AOI measurement is also the first exploitation for target localization. Furthermore, the estimate combination rule based on the estimation covariance is used in the DCTLS algorithm, which can represent the confidence of estimate results transmitted from neighbors, thus generating the localization performance improvement.

REMARK 5 The DCTLS algorithm using the BR and AOI measurements provides the equivalent efficacy to the conventional localization algorithms using the BR and AOA measurements [28], [29], [30], [31]. This indicates that the distributed localization can be extended to the cases of the BR and AOA measurements. Their different system architectures determine that they can be applied for different scenarios. But it is noteworthy that in many applications, where the receivers are placed on lightweight platforms (such as UAVs), the directional receivers cannot be used and the AOA measurements are not available, and thus the hybrid BR and AOA localization algorithm is inapplicable.

REMARK 6 The system structure of the DCTLS algorithm has no centralized fusion center but each receiver acts as a fusion center to perform the processes of local localization and estimate combination, where each receiver bears the efficacy of traditional centralized localization methods. The DCTLS algorithm provides desirable robustness to single-point failure, which implies that the radar system can perform the localization task unless all transmitters and receivers are inoperable.

REMARK 7 Compared with the distributed localization algorithms in other fields [37], [38], [39], where the number of neighbors of each node generally needs to meet a specific minimum condition (more than one), the DCTLS algorithm for each receiver does not suffer from this limitation, even it can estimate the target position independently and does not require any information of other receivers. Generally, the DCTLS algorithm with partially connected receivers provides reasonably worse performance than that with completely connected receivers, but the latter suffers from larger computational and communication burdens. When the number and topology of receivers are fixed, the addition of transmitters can naturally bring about a accuracy gain.

REMARK 8 The DCTLS algorithm can be applicable for multiple targets when all targets are sufficiently separated in space to require different probing beams for illumination. When there are multiple targets in a transmission beam, the data association method presented in [45] can be adopted to associate measurement vectors for different targets. Then, the positions of multiple targets can be estimated using the DCTLS algorithm independently.

The developed distributed localization framework with no centralized fusion center reduces the communication burdens among receivers, but it increases the communication burdens between transmitters and receivers when the AOI measurements are obtained by transmitters and receivers cooperatively. In addition, the proposed method is applicable when all transmitters and receivers are fully cooperative.

C. Performance Analysis

Generally, the CRLB [42] determines a theoretical performance bound that the estimator can achieve. We also derive the CRLB for the proposed DCTLS algorithm for theoretical analysis. Since the DCTLS algorithm consists of the steps of local localization and estimate combination, we first derive the CRLB for local localization and then use the estimate combination rule to obtain the final CRLB of each receiver for target localization.

For local localization of any receiver $n \in \mathcal{R}$, the CRLB matrix is defined [42] as follows:

$$\mathbf{C}_n = \mathbf{J}_n^{-1} \tag{41}$$

where $\mathbf{J}_n$ is the Fisher information matrix (FIM), which is derived by

$$\mathbf{J}_n = (\nabla_{\mathbf{x}}^{\mathbf{z}_n})^{\mathrm{T}} \mathbf{Q}_n^{-1} \nabla_{\mathbf{x}}^{\mathbf{z}_n} \tag{42}$$

where $\nabla_{\mathbf{x}}^{\mathbf{z}_n}$ is the Jacobian matrix of measurement vector $\mathbf{z}_n$ regarding estimation variable $\mathbf{x}$ as follows:

$$\nabla_{\mathbf{x}}^{\mathbf{z}_n} = \left[\left(\frac{\partial \mathbf{z}_{d,n}}{\partial \mathbf{x}^{\mathrm{T}}} \right)^{\mathrm{T}}, \left(\frac{\partial \mathbf{z}_{\phi,n}}{\partial \mathbf{x}^{\mathrm{T}}} \right)^{\mathrm{T}}, \left(\frac{\partial \mathbf{z}_{\theta,n}}{\partial \mathbf{x}^{\mathrm{T}}} \right)^{\mathrm{T}} \right]^{\mathrm{T}} \tag{43}$$

with

$$\frac{\partial \mathbf{z}_{d,n}}{\partial \mathbf{x}^{\mathrm{T}}} = \begin{bmatrix} (\mathbf{x}-\mathbf{t}_1)^{\mathrm{T}}/d_{T,1} + (\mathbf{x}-\mathbf{r}_n)^{\mathrm{T}}/d_{R,n} \\ (\mathbf{x}-\mathbf{t}_2)^{\mathrm{T}}/d_{T,2} + (\mathbf{x}-\mathbf{r}_n)^{\mathrm{T}}/d_{R,n} \\ \vdots \\ (\mathbf{x}-\mathbf{t}_M)^{\mathrm{T}}/d_{T,M} + (\mathbf{x}-\mathbf{r}_n)^{\mathrm{T}}/d_{R,n} \end{bmatrix} \tag{44a}$$

$$\frac{\partial \mathbf{z}_{\phi,n}}{\partial \mathbf{x}^{\mathrm{T}}} = \begin{bmatrix} -\mathbf{v}_{1,n}^{\mathrm{T}}/(d_{T,1}\cos\theta_{1,n}) \\ -\mathbf{v}_{2,n}^{\mathrm{T}}/(d_{T,2}\cos\theta_{2,n}) \\ \vdots \\ -\mathbf{v}_{M,n}^{\mathrm{T}}/(d_{T,M}\cos\theta_{M,n}) \end{bmatrix} \tag{44b}$$

$$\frac{\partial \mathbf{z}_{\theta,n}}{\partial \mathbf{x}^{\mathrm{T}}} = \begin{bmatrix} -\mathbf{w}_{1,n}^{\mathrm{T}}/d_{T,1} \\ -\mathbf{w}_{2,n}^{\mathrm{T}}/d_{T,2} \\ \vdots \\ -\mathbf{w}_{M,n}^{\mathrm{T}}/d_{T,M} \end{bmatrix}. \tag{44c}$$

Note that the derived FIM $\mathbf{J}_n$ is different from that of the hybrid BR and AOA localization [29], since the different BR and AOI measurements are used in this work.

Finally, based on the assumption that the measured information from different receivers is independent [46], [47], the combined FIM for receiver n is obtained as follows:

$$\mathbf{J}_n = \sum_{i \in \mathcal{R}_n} (\nabla_{\mathbf{x}}^{\mathbf{z}_i})^{\mathrm{T}} (\mathbf{Q}_i)^{-1} \nabla_{\mathbf{x}}^{\mathbf{z}_i}. \tag{45}$$

Based on the derived FIM, different performance measure criteria [48] can be adopted to evaluate the target localization performance for receiver n, such as the D-optimality criterion [48] that can be equivalent to the determinant of the FIM. Based on the D-optimality criterion, the following proposition demonstrates the performance relationship between the proposed DCTLS algorithm and its centralized counterpart.

PROPOSITION 3 When the AOI measurements are obtained by all transmitters themselves, i.e., the AOI measurements are independent to all receivers, the DCTLS algorithm provides better localization performance than the centralized counterpart when the following condition is satisfied

$$N_n \left(\left(\frac{\partial \mathbf{z}_\phi}{\partial \mathbf{x}^{\mathrm{T}}} \right)^{\mathrm{T}} \mathbf{Q}_\phi^{-1} \frac{\partial \mathbf{z}_\phi}{\partial \mathbf{x}^{\mathrm{T}}} + \left(\frac{\partial \mathbf{z}_\theta}{\partial \mathbf{x}^{\mathrm{T}}} \right)^{\mathrm{T}} \mathbf{Q}_\theta^{-1} \frac{\partial \mathbf{z}_\theta}{\partial \mathbf{x}^{\mathrm{T}}} \right)$$

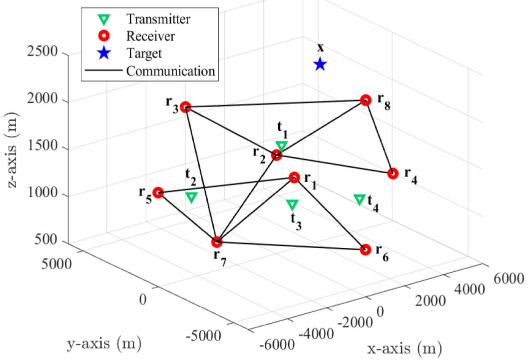

Fig. 6. Simulation scenario of MIMO radar for target localization.

$$\succ \sum_{i \in \mathcal{R} \setminus \mathcal{R}_n} \left(\frac{\partial \mathbf{z}_{d,i}}{\partial \mathbf{x}^{\mathrm{T}}} \right)^{\mathrm{T}} \mathbf{Q}_{d,i}^{-1} \frac{\partial \mathbf{z}_{d,i}}{\partial \mathbf{x}^{\mathrm{T}}} \tag{46}$$

where $\mathbf{A} \succ \mathbf{B}$ indicates that $\mathbf{A} - \mathbf{B}$ is a positive definite matrix and N_n is the cardinality of neighbor set $\mathcal{N}_n$ for receiver n. When the AOI measurements are obtained by all transmitters and all receivers cooperatively, the DCTLS algorithm generally provides worse localization performance than the centralized one, but they provide the same performance when the network architecture with complete connectivity for all receivers is considered in the DCTLS algorithm.

PROOF See Appendix 4. ■

It is noteworthy that the superiority of the DCTLS algorithm over the centralized counterpart only holds when all transmitters have both transmitting and receiving functions. In this case, MN BR measurements, M azimuth measurements, and M elevation measurements are used in the centralized method for target localization. However, since any receiver n combines local localization results from its neighbors in the DCTLS algorithm, it totally uses $M(N_n+1)$ BR measurements, $M(N_n+1)$ azimuth measurements, and $M(N_n+1)$ elevation measurements for target localization. Although N_n+1 is generally smaller than N for BR measurements, more information of MN_n azimuth measurements and MN_n elevation measurements in the DCTLS algorithm may make up or even exceed the information deficit in BR measurements compared with the centralized method.

IV. SIMULATION RESULTS

In this section, some numerical simulations are performed to validate the effectiveness of the proposed DCTLS algorithm for target localization. The simulation scenario is depicted in Fig. 6, where the MIMO radar constitutes with widely separated four transmitters and partially connected eight receivers to estimate the target position appearing in the surveillance area of the radar system. The positions of all transmitters, receivers, and the target are provided in Table I. To model the uncertainty of the positions of transmitters and receivers, the position of each transmitter or each receiver given in Table I is contaminated by a zero-mean Gaussian

TABLE I
Simulation Parameters of Positions of Transmitters, Receivers, and Target

Symbol	Definition	Value
$\mathbf{t}_1$	Position of transmitter 1	$[-2000\mathrm{m}, -3000\mathrm{m}, 2000\mathrm{m}]^{\mathrm{T}}$
$\mathbf{t}_2$	Position of transmitter 2	$[-2000\mathrm{m}, 3000\mathrm{m}, 1000\mathrm{m}]^{\mathrm{T}}$
$\mathbf{t}_3$	Position of transmitter 3	$[2000\mathrm{m}, 1500\mathrm{m}, 800\mathrm{m}]^{\mathrm{T}}$
$\mathbf{t}_4$	Position of transmitter 4	$[2000\mathrm{m}, -3000\mathrm{m}, 1200\mathrm{m}]^{\mathrm{T}}$
$\mathbf{r}_1$	Position of receiver 1	$[-4500\mathrm{m}, -4500\mathrm{m}, 1800\mathrm{m}]^{\mathrm{T}}$
$\mathbf{r}_2$	Position of receiver 2	$[3500\mathrm{m}, 4500\mathrm{m}, 1000\mathrm{m}]^{\mathrm{T}}$
$\mathbf{r}_3$	Position of receiver 3	$[0, 6000\mathrm{m}, 1600\mathrm{m}]^{\mathrm{T}}$
$\mathbf{r}_4$	Position of receiver 4	$[6000\mathrm{m}, 0, 1000\mathrm{m}]^{\mathrm{T}}$
$\mathbf{r}_5$	Position of receiver 5	$[-6000\mathrm{m}, 0, 1500\mathrm{m}]^{\mathrm{T}}$
$\mathbf{r}_6$	Position of receiver 6	$[0, -6000\mathrm{m}, 1000\mathrm{m}]^{\mathrm{T}}$
$\mathbf{r}_7$	Position of receiver 7	$[-3000\mathrm{m}, 0, 800\mathrm{m}]^{\mathrm{T}}$
$\mathbf{r}_8$	Position of receiver 8	$[5000\mathrm{m}, 500\mathrm{m}, 1800\mathrm{m}]^{\mathrm{T}}$
$\mathbf{x}$	Position of the target	$[1500\mathrm{m}, -1000\mathrm{m}, 2500\mathrm{m}]^{\mathrm{T}}$

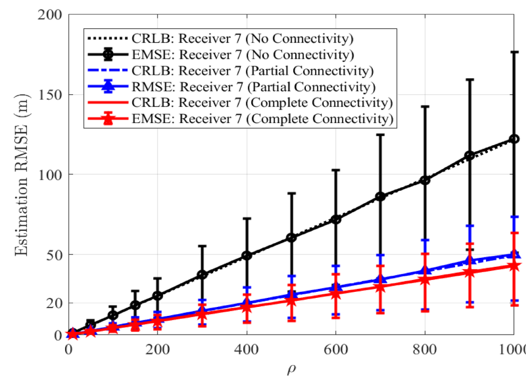

Fig. 7. Estimation RMSEs and CRLBs of receiver 7 with different connectivity using the DCTLS algorithm for target localization with different values of ρ.

noise with covariance $\sigma^2 \mathbf{I}_3$, where $\sigma^2 = 100$. The task of the MIMO radar is to estimate the unknown target position by using the obtained measurements. The estimation root mean square error (RMSE) is used to evaluate localization performance, which is defined as follows:

$$\mathrm{RMSE} = \sqrt{\frac{1}{N_{\mathrm{MC}}} \sum_{i=1}^{N_{\mathrm{MC}}} \|\hat{\mathbf{x}}_i - \mathbf{x}\|^2} \tag{47}$$

where $\hat{\mathbf{x}}_i$ is the estimated target position at ith trial and $N_{\mathrm{MC}} = 1000$ is the number of Monte-Carlo trials. In the following simulations, the efficacy and superiority of the proposed DCTLS algorithm are validated, respectively.

A. Efficacy Verification

The efficacy of the proposed DCTLS algorithm for target localization under different levels of the measurement error is first validated. The covariance matrix of the measurement error for receiver n $(n = 1, 2, \ldots, 8)$ is set by $\mathbf{Q}_n = \mathrm{blkdiag}\{\sigma_{d,n}^2 \mathbf{I}_4, \sigma_{\phi,n}^2 \mathbf{I}_4, \sigma_{\theta,n}^2 \mathbf{I}_4\}$ with $\sigma_{d,n} = \rho \times 1\mathrm{m}$, $\sigma_{\phi,n} = \sigma_{\theta,n} = \rho \times 0.002^\circ$, and ρ representing the level of the measurement error. To validate the efficacy of the DCTLS algorithm for all cases of the network architecture shown in Fig. 2, apart from the scenario of receivers with partial connectivity shown in Fig. 6, the scenarios of receivers with complete connectivity and no connectivity

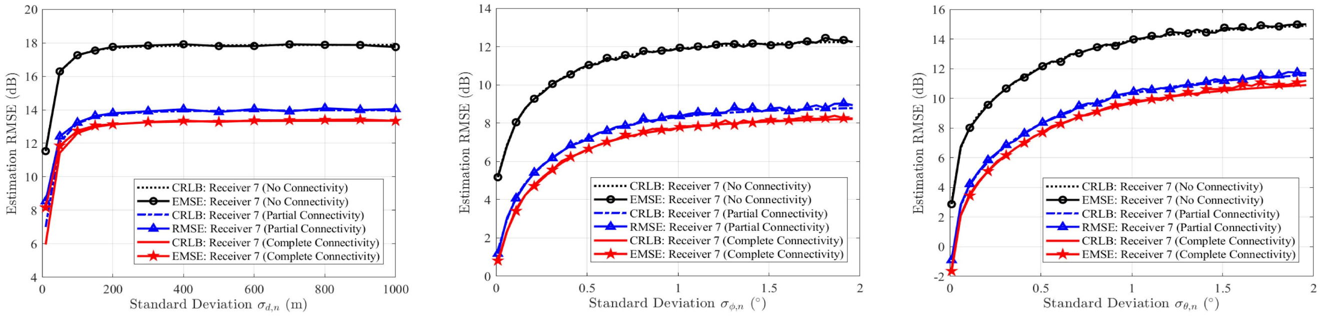

(a) (b) (c)

Fig. 8. Estimation RMSEs and CRLBs of receiver 7 with different connectivity using the DCTLS algorithm for target localization with different levels of BR, azimuth, and elevation measurement errors: (a) different levels of BR measurement error; (b) different levels of azimuth measurement error; (c) different levels of elevation measurement error.

are also considered for simulation. The estimation RMSEs and CRLBs of receiver 7 with different connectivity using the DCTLS algorithm to estimate the target position with the values of ρ being 10 to 1000 are shown in Fig. 7. The RMSEs and CRLBs of other receivers are not shown in Fig. 7 for brevity. The confidence intervals with the degree of confidence 95% for the three cases are also shown in Fig. 7. From Fig. 7, we see that the receiver with different connectivity can achieve its CRLBs for different values of ρ, and the receiver with complete connectivity provides the best performance while the receiver with no connectivity provides the worst performance. This is not surprising because the receiver with more neighbors can obtain more useful information for performance improvement. To validate the efficacy of the proposed DCTLS algorithm for target localization under different levels of the BR, azimuth, and elevation measurement errors, the following three cases are considered for simulation: 1) $\sigma_{\phi,n} = \sigma_{\theta,n} = 1^\circ$, and $\sigma_{d,n} = \rho \times 1$m with the values of ρ being 10 to 1000; 2) $\sigma_{d,n} = 50$m, $\sigma_{\theta,n} = 0.1^\circ$, and $\sigma_{\phi,n} = \rho \times 1^\circ$ with the values of ρ being 0.01 to 2; 3) $\sigma_{d,n} = 50$m, $\sigma_{\phi,n} = 0.1^\circ$, and $\sigma_{\theta,n} = \rho \times 1^\circ$ with the values of ρ being 0.01 to 2. The estimation RMSEs and CRLBs of receiver 7 with different connectivity using the proposed DCTLS algorithm for target localization in these three cases are shown in Fig. 8(a)–(c), respectively. It can be seen from Fig. 8 that the receiver with different connectivity using the DCTLS algorithm can achieve its CRLBs for target localization with different levels of the BR, azimuth, and elevation measurement errors, respectively. All these results demonstrate the efficacy of the DCTLS algorithm.

B. Performance Comparison

Next, the performance comparison of the proposed DCTLS algorithm using the BR and AOI measurements (named the DCTLS BR/AOI) with other typical algorithms for target localization is performed. In the considered distributed localization scenario with no centralized fusion center, all the conventional centralized localization algorithms cannot be applicable. However, to illustrate the superiority of the DCTLS BR/AOI sufficiently, the centralized BR algorithm [17], the centralized BR/AOA algorithm [29], and the centralized BR/AOI algorithm using the same method as in the centralized BR/AOA algorithm are chosen as counterparts of the DCTLS BR/AOI. Note that all these three centralized algorithms combine measurements from all receivers and use the centralized WLS (CWLS) algorithm to estimate the target position, and thus they are named the CWLS BR, the CWLS BR/AOA, and the CWLS BR/AOI, respectively. It is assumed that there exists a centralized fusion center in the radar system for these three algorithms, and assumed that all receivers can obtain the AOA measurements for the CWLS BR/AOA. In addition, the distributed LS (DLS) BR/AOI using the conventional LS method (27) for local localization is also chosen as the counterpart of the DCTLS BR/AOI. For the CWLS BR/AOI, the DLS BR/AOI, and the DCTLS BR/AOI, all AOI measurements are obtained by all transmitters themselves and then are transmitted to all receivers. For fair comparison, the same settings as in Figs. 7 and 8 are used for all the compared algorithms, and the same level of the AOA measurement error as that of the AOI measurement error is set for the CWLS BR/AOA.

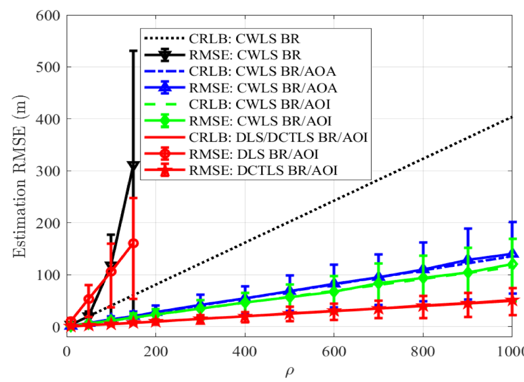

Fig. 9. Comparison results of all algorithms in terms of estimation RMSE and CRLB for target localization with different values of ρ.

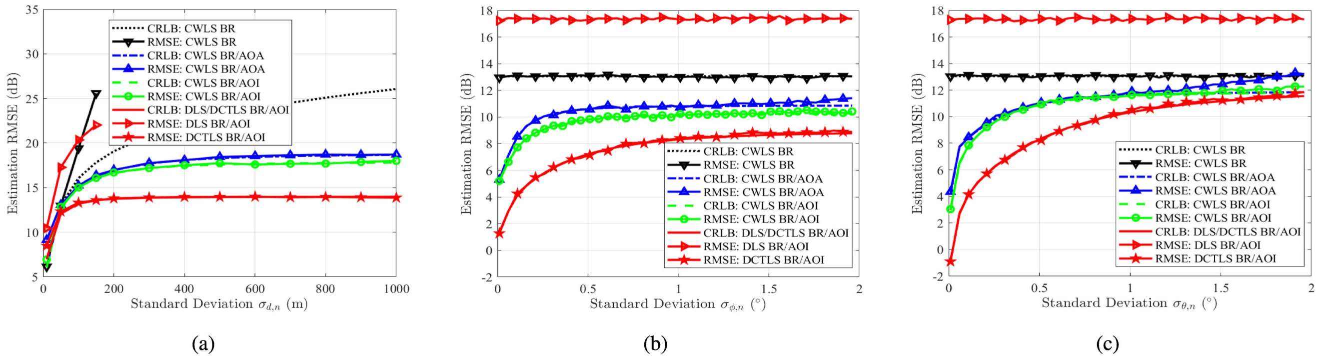

Fig. 10. Comparison results of all algorithms in terms of estimation RMSEs and CRLBs for target localization with different levels of BR, azimuth, and elevation measurement errors: (a) different levels of BR measurement error; (b) different levels of azimuth measurement error; (c) different levels of elevation measurement error.

Using the same simulation settings as in Fig. 7, the estimation RMSEs and CRLBs of all algorithms for target localization with the values of ρ being 10 to 1000 are shown in Fig. 9, where only the simulation results of receiver 7 using the proposed DCTLS BR/AOI are shown in the figure for brevity, and only the relatively small estimation RMSEs of the DLS BR/AOI and the CWLS BR are shown since these two algorithms are divergent when the value of ρ exceeds 150. From Fig. 9, we see that the DCTLS BR/AOI provides the best performance in all the compared algorithms. The CWLS BR/AOA provides better performance than the CWLS BR unsurprisingly since the former utilizes more AOA measurements than the latter to estimate the target position, we also see that the RMSEs of the CWLS BR deviate the CRLBs when the level of the measurement error is high because the limited BR measurements are used. The DLS BR/AOI provides poor performance since it does not consider the error in the data matrix. Although it is shown from Fig. 9 that the CWLS BR/AOI provides slightly better performance than the CWLS BR/AOA, we cannot conclude that the former is superior to the latter. Actually, the CWLS BR/AOI and the CWLS BR/AOA are suitable for different application scenarios. The DCTLS BR/AOI with an estimate combination rule considers the importance of estimation results from different neighbors, and thus it can provide the performance gain over the centralized algorithms using raw measurements once time for target localization, which verifies Proposition 3.

Finally, we consider the three simulation scenarios as in Fig. 8 for performance comparison of the proposed DCTLS BR/AOI with other algorithms. The comparison results of all algorithms in terms of the estimation RMSE and CRLB for target localization in these three scenarios are shown in Fig. 10(a)–(c), respectively. Here, only the relatively small estimation RMSEs of the DLS BR/AOI and the CWLS BR are shown in Fig. 10(a) since these two algorithms are divergent when the value of $\sigma_{d,n}$ exceeds 150 m. As can be seen from Fig. 10(a), the DCTLS BR/AOI can provide better performance than all the compared algorithms in different levels of the BR measurement errors. The CWLS BR suffers from performance degradation significantly when the level of the BR measurement error is high. As can be seen from Fig. 10(b) and (c), the DCTLS BR/AOI can also provide better performance than all the compared algorithms in different levels of the azimuth and elevation measurement errors, and the localization performance of the CWLS BR remains unchanged since this algorithm is independent of angular measurements. We also see from Fig. 10(b) and (c) that the azimuth and the elevation have different effects on the localization performance. In addition, the DLS BR/AOI provides the worst performance compared with all other algorithms in Fig. 10(a)–(c) since the error in the data matrix is ignored by this algorithm. Furthermore, the DCTLS BR/AOI outperforms the CWLS BR/AOI since the DCTLS BR/AOI utilizes the information of the AOI measurement many times but the CWLS BR/AOI utilizes the information of the AOI measurement only once.

From all above simulation results, we can conclude that the proposed DCTLS algorithm using BR and AOI measurements can provide the desirable localization efficacy for the MIMO radar with widely separated directional transmitters and omnidirectional receivers as well as no centralized fusion center, and can provide the significant performance superiority over the conventional localization algorithms.

V. CONCLUSION

This article considers the MIMO radar with widely separated directional transmitters and omnidirectional receivers generating the BR and AOI measurements for target localization. The distributed localization framework with no centralized fusion center is developed for receivers of the MIMO radar and the localization problem is formulated as solving a linear matrix equation. The DCTLS algorithm is therefore proposed to solve this problem. The performance analysis of the DCTLS algorithm in terms of the CRLB is further performed. Simulation results demonstrate that the localization performance of the DCTLS algorithm can match with the CRLB and is superior to the other typical algorithms. In the future work, the localization and data association methods will be studied for multiple targets with false alarms.

APPENDIX 1

Proof of Proposition 1

Taking the tangent of azimuth ϕ_m defined in (2) gives

$$y = x\tan\phi_m - x_{T,m}\tan\phi_m + y_{T,m}. \tag{48}$$

In addition, according to the geometry of the receiver, transmitter, and target, one can obtain

$$\sqrt{(x-x_{R,n})^2 + (y-y_{R,n})^2} = d_{m,n} - \frac{y-y_{T,m}}{\sin\phi_m}. \tag{49}$$

The square of both sides of (49) is given by

$$\begin{aligned}(x-x_{R,n})^2 + (y-y_{R,n})^2 &= d_{m,n}^2 + \frac{(y-y_{T,m})^2}{\sin^2\phi_m}\\ &\quad - 2d_{m,n}\frac{y-y_{T,m}}{\sin\phi_m}.\end{aligned} \tag{50}$$

Substituting (48) into (50) and after several manipulations give the result of x. Then, substituting the result of x into (48) gives the result of y. For the derivation of z, taking the tangent of elevation θ_m defined in (3) and after some manipulations give

$$\begin{aligned}z &= z_{T,m} + (x-x_{T,m})\cos\phi_m\tan\theta_m\\ &\quad + (y-y_{T,m})\sin\phi_m\tan\theta_m.\end{aligned} \tag{51}$$

Substituting the results of x and y into (51) gives the result of z. The analytical results of x, y, and z are given in (52), (53), and (54), respectively. That is, by using a pair of exactly known BR $d_{m,n}$, azimuth ϕ_m, and elevation θ_m, the target position can be uniquely determined.

$$\begin{aligned}x &= x_{T,m}\\ &\quad + \frac{d_{m,n}^2 - \|\mathbf{t}_m - \mathbf{r}_n\|^2}{2(x_{T,m} - x_{R,n} + (y_{T,m} - y_{R,n})\tan\phi_m + d_{m,n}\sec\phi_m)}\end{aligned} \tag{52}$$

$$\begin{aligned}y &= y_{T,m}\\ &\quad + \frac{\tan\phi_m(d_{m,n}^2 - \|\mathbf{t}_m - \mathbf{r}_n\|^2)}{2(x_{T,m} - x_{R,n} + (y_{T,m} - y_{R,n})\tan\phi_m + d_{m,n}\sec\phi_m)}\end{aligned} \tag{53}$$

$$\begin{aligned}z &= z_{T,m}\\ &\quad + \frac{\tan\theta_m(d_{m,n}^2 - \|\mathbf{t}_m - \mathbf{r}_n\|^2)}{2\cos\phi_m(x_{T,m} - x_{R,n} + (y_{T,m} - y_{R,n})\tan\phi_m + d_{m,n}\sec\phi_m)}.\end{aligned} \tag{54}$$

APPENDIX 2

Derivation of Equation (29)

For convenience of computation, data matrix $\mathbf{A}_n$ can be written as $\mathbf{A}_n = [\mathbf{a}_n^1, \mathbf{a}_n^2, \mathbf{a}_n^3]$ with

$$\begin{aligned}\mathbf{a}_n^1 = \Big[&2d_{1,n}\cos\phi_{1,n}\cos\theta_{1,n} + 2x_{T,1} - 2x_{R,n}\\ &2d_{2,n}\cos\phi_{2,n}\cos\theta_{2,n} + 2x_{T,2} - 2x_{R,n}, \ldots\\ &2d_{M,n}\cos\phi_{M,n}\cos\theta_{M,n} + 2x_{T,M} - 2x_{R,n}\\ &\sin\phi_{1,n}, \sin\phi_{2,n}, \ldots, \sin\phi_{M,n}\\ &\cos\phi_{1,n}\sin\theta_{1,n}, \cos\phi_{2,n}\sin\theta_{2,n}, \ldots,\\ &\cos\phi_{M,n}\sin\theta_{M,n}\Big]^{\mathrm{T}}\end{aligned}$$

$$\begin{aligned}\mathbf{a}_n^2 = \Big[&2d_{1,n}\sin\phi_{1,n}\cos\theta_{1,n} + 2y_{T,1} - 2y_{R,n}\\ &2d_{2,n}\sin\phi_{2,n}\cos\theta_{2,n} + 2y_{T,2} - 2y_{R,n}, \ldots\\ &2d_{M,n}\sin\phi_{M,n}\cos\theta_{M,n} + 2y_{T,M} - 2y_{R,n}\\ &-\cos\phi_{1,n}, -\cos\phi_{2,n}, \ldots, -\cos\phi_{M,n}\\ &\sin\phi_{1,n}\sin\theta_{1,n}, \sin\phi_{2,n}\sin\theta_{2,n}, \ldots, \sin\phi_{M,n}\sin\theta_{M,n}\Big]^{\mathrm{T}}\end{aligned}$$

$$\begin{aligned}\mathbf{a}_n^3 = [&2d_{1,n}\sin\theta_{1,n} + 2z_{T,1} - 2z_{R,n}\\ &2d_{2,n}\sin\theta_{2,n} + 2z_{T,2} - 2z_{R,n}, \ldots\\ &2d_{M,n}\sin\theta_{M,n} + 2z_{T,M} - 2z_{R,n}\\ &\mathbf{0}_M^{\mathrm{T}}, -\cos\theta_{1,n}, -\cos\theta_{2,n}, \ldots, -\cos\theta_{M,n}]^{\mathrm{T}}.\end{aligned}$$

Thus, taking the Taylor expansion of $\mathbf{A}_n = \mathbf{A}(\mathbf{z}_n)$ around $\tilde{\mathbf{z}}_n$ and ignoring the second-order and higher-order terms give

$$\begin{aligned}\mathbf{A}(\mathbf{z}_n) &\approx \mathbf{A}(\tilde{\mathbf{z}}_n) + \frac{\partial\mathbf{A}(\tilde{\mathbf{z}}_n)}{\partial\tilde{\mathbf{z}}_n^{\mathrm{T}}}(\mathbf{z}_n - \tilde{\mathbf{z}}_n)\\ &= \mathbf{A}(\tilde{\mathbf{z}}_n) - \frac{\partial\mathbf{A}(\tilde{\mathbf{z}}_n)}{\partial\tilde{\mathbf{z}}_n^{\mathrm{T}}}\mathbf{n}_n\\ &= \mathbf{A}(\tilde{\mathbf{z}}_n) - \left[\frac{\partial\mathbf{a}_n^1}{\partial\tilde{\mathbf{z}}_n^{\mathrm{T}}}\mathbf{n}_n, \frac{\partial\mathbf{a}_n^2}{\partial\tilde{\mathbf{z}}_n^{\mathrm{T}}}\mathbf{n}_n, \frac{\partial\mathbf{a}_n^3}{\partial\tilde{\mathbf{z}}_n^{\mathrm{T}}}\mathbf{n}_n\right]\\ &= \mathbf{A}(\tilde{\mathbf{z}}_n) - [\mathbf{G}_n^1\mathbf{n}_n, \mathbf{G}_n^2\mathbf{n}_n, \mathbf{G}_n^3\mathbf{n}_n]\\ &= \tilde{\mathbf{A}}_n - \Delta\mathbf{A}_n\end{aligned} \tag{55}$$

where matrices $\mathbf{G}_n^1$, $\mathbf{G}_n^2$, and $\mathbf{G}_n^3$ are the Jacobian matrices of $\mathbf{a}_n^1(\tilde{\mathbf{z}}_n)$, $\mathbf{a}_n^2(\tilde{\mathbf{z}}_n)$, and $\mathbf{a}_n^3(\tilde{\mathbf{z}}_n)$ with respect to $\tilde{\mathbf{z}}_n$ given by

$$\left\{\begin{aligned}\mathbf{G}_n^1 &= \begin{bmatrix}\mathbf{G}_1^{11} & \mathbf{G}_1^{12} & \mathbf{G}_1^{13}\\ \mathbf{O}_{M\times M} & \mathbf{G}_1^{22} & \mathbf{O}_{M\times M}\\ \mathbf{O}_{M\times M} & \mathbf{G}_1^{32} & \mathbf{G}_1^{33}\end{bmatrix}\\ \mathbf{G}_1^{11} &= \mathrm{diag}\left\{2\cos\phi_{1,n}\cos\theta_{1,n}, 2\cos\phi_{2,n}\cos\theta_{2,n}, \ldots,\right.\\ &\qquad\left. 2\cos\phi_{M,n}\cos\theta_{M,n}\right\}\\ \mathbf{G}_1^{12} &= \mathrm{diag}\left\{-2d_{1,n}\sin\phi_{1,n}\cos\theta_{1,n},\right.\\ &\qquad -2d_{2,n}\sin\phi_{2,n}\cos\theta_{2,n}, \ldots,\\ &\qquad\left. -2d_{M,n}\sin\phi_{M,n}\cos\theta_{M,n}\right\}\\ \mathbf{G}_1^{13} &= \mathrm{diag}\{-2d_{1,n}\cos\phi_{1,n}\sin\theta_{1,n},\\ &\qquad -2d_{2,n}\cos\phi_{2,n}\sin\theta_{2,n}, \ldots,\\ &\qquad -2d_{M,n}\cos\phi_{M,n}\sin\theta_{M,n}\}\\ \mathbf{G}_1^{22} &= \mathrm{diag}\left\{\cos\phi_{1,n}, \cos\phi_{2,n}, \ldots, \cos\phi_{M,n}\right\}\\ \mathbf{G}_1^{32} &= \mathrm{diag}\left\{-\sin\phi_{1,n}\sin\theta_{1,n}, -\sin\phi_{2,n}\sin\theta_{2,n}, \ldots,\right.\\ &\qquad\left. -\sin\phi_{M,n}\sin\theta_{M,n}\right\}\\ \mathbf{G}_1^{33} &= \mathrm{diag}\left\{\cos\phi_1\cos\theta_{1,n}, \cos\phi_{2,n}\cos\theta_{2,n},\right.\\ &\qquad\left. \ldots, \cos\phi_{M,n}\cos\theta_{M,n}\right\}\end{aligned}\right. , \tag{56}$$

$$\begin{cases} \mathbf{G}_n^2 = \begin{bmatrix} \mathbf{G}_2^{11} & \mathbf{G}_2^{12} & \mathbf{G}_2^{13} \\ \mathbf{O}_{M\times M} & \mathbf{G}_2^{22} & \mathbf{O}_{M\times M} \\ \mathbf{O}_{M\times M} & \mathbf{G}_2^{32} & \mathbf{G}_2^{33} \end{bmatrix} \\ \mathbf{G}_2^{11} = \mathrm{diag}\left\{2\sin\phi_{1,n}\cos\theta_{1,n}, 2\sin\phi_{2,n}\cos\theta_{2,n}, \ldots, \right. \\ \qquad \left. 2\sin\phi_{M,n}\cos\theta_{M,n}\right\} \\ \mathbf{G}_2^{12} = \mathrm{diag}\left\{2d_{1,n}\cos\phi_{1,n}\cos\theta_{1,n}, 2d_{2,n}\cos\phi_{2,n}\cos\theta_{2,n}, \right. \\ \qquad \left. \ldots, 2d_{M,n}\cos\phi_{M,n}\cos\theta_{M,n}\right\} \\ \mathbf{G}_2^{13} = \mathrm{diag}\left\{-2d_{1,n}\sin\phi_{1,n}\sin\theta_{1,n}, \right. \\ \qquad -2d_{2,n}\sin\phi_{2,n}\sin\theta_{2,n}, \ldots, \\ \qquad \left. -\, 2d_{M,n}\sin\phi_{M,n}\sin\theta_{M,n}\right\} \\ \mathbf{G}_2^{22} = \mathrm{diag}\left\{\sin\phi_{1,n}, \sin\phi_{2,n}, \ldots, \sin\phi_{M,n}\right\} \\ \mathbf{G}_2^{32} = \mathrm{diag}\left\{\cos\phi_{1,n}\sin\theta_{1,n}, \cos\phi_{2,n}\sin\theta_{2,n}, \ldots, \right. \\ \qquad \left. \cos\phi_{M,n}\sin\theta_{M,n}\right\} \\ \mathbf{G}_2^{33} = \mathrm{diag}\left\{\sin\phi_{1,n}\cos\theta_{1,n}, \sin\phi_{2,n}\cos\theta_{2,n}, \ldots, \right. \\ \qquad \left. \sin\phi_{M,n}\cos\theta_{M,n}\right\} \end{cases} \tag{57}$$

$$\begin{cases} \mathbf{G}_n^3 = \begin{bmatrix} \mathbf{G}_3^{11} & \mathbf{O}_{M\times M} & \mathbf{G}_3^{13} \\ \mathbf{O}_{M\times M} & \mathbf{O}_{M\times M} & \mathbf{O}_{M\times M} \\ \mathbf{O}_{M\times M} & \mathbf{O}_{M\times M} & \mathbf{G}_3^{33} \end{bmatrix} \\ \mathbf{G}_3^{11} = \mathrm{diag}\left\{2\sin\theta_{1,n}, 2\sin\theta_{2,n}, \ldots, 2\sin\theta_{M,n}\right\} \\ \mathbf{G}_3^{13} = \mathrm{diag}\left\{2d_{1,n}\cos\theta_{1,n}, 2d_{2,n}\cos\theta_{2,n}, \ldots, \right. \\ \qquad \left. 2d_{M,n}\cos\theta_{M,n}\right\} \\ \mathbf{G}_3^{33} = \mathrm{diag}\left\{\sin\theta_{1,n}, \sin\theta_{2,n}, \ldots, \sin\theta_{M,n}\right\} \end{cases} \tag{58}$$

where $\mathbf{O}_{m\times n}$ is an $m \times n$ matrix whose all elements are 0.

For data vector $\mathbf{b}_n = \mathbf{b}(\mathbf{z}_n)$, taking its Taylor expansion and ignoring the second-order and higher-order terms give

$$\begin{aligned} \mathbf{b}(\mathbf{z}_n) &\approx \mathbf{b}(\tilde{\mathbf{z}}_n) + \frac{\partial \mathbf{b}(\tilde{\mathbf{z}}_n)}{\partial \tilde{\mathbf{z}}_n^{\mathrm{T}}}(\mathbf{z}_n - \tilde{\mathbf{z}}_n) \\ &= \mathbf{b}(\tilde{\mathbf{z}}_n) - \frac{\partial \mathbf{b}(\tilde{\mathbf{z}}_n)}{\partial \tilde{\mathbf{z}}_n^{\mathrm{T}}}\mathbf{n}_n \\ &= \mathbf{b}(\tilde{\mathbf{z}}_n) - \mathbf{G}_n^4\mathbf{n}_n \\ &= \tilde{\mathbf{b}}_n - \Delta\mathbf{b}_n \end{aligned} \tag{59}$$

where matrix $\mathbf{G}_n^4$ is the Jacobian matrix of $\mathbf{b}(\tilde{\mathbf{z}}_n)$ with respect to $\tilde{\mathbf{z}}_n$ given by

$$\begin{cases} \mathbf{G}_n^4 = \begin{bmatrix} \mathbf{G}_4^{11} & \mathbf{G}_4^{12} & \mathbf{G}_4^{13} \\ \mathbf{O}_{M\times M} & \mathbf{G}_4^{22} & \mathbf{O}_{M\times M} \\ \mathbf{O}_{M\times M} & \mathbf{G}_4^{32} & \mathbf{G}_4^{33} \end{bmatrix} \\ \mathbf{G}_4^{11} = \mathrm{diag}\{2d_{1,n} + 2\mathbf{u}_{1,n}^{\mathrm{T}}\mathbf{t}_1, 2d_{2,n} + 2\mathbf{u}_{2,n}^{\mathrm{T}}\mathbf{t}_2, \\ \qquad \cdots, 2d_{M,n} + 2\mathbf{u}_{M,n}^{\mathrm{T}}\mathbf{t}_M\} \\ \mathbf{G}_4^{12} = \mathrm{diag}\{2d_{1,n}\nabla_\phi\mathbf{u}_{1,n}^{\mathrm{T}}\mathbf{t}_1, 2d_{2,n}\nabla_\phi\mathbf{u}_{2,n}^{\mathrm{T}}\mathbf{t}_2, \\ \qquad \cdots, 2d_{M,n}\nabla_\phi\mathbf{u}_{M,n}^{\mathrm{T}}\mathbf{t}_M\} \\ \nabla_\phi\mathbf{u}_{m,n} = [-\sin\phi_{m,n}\cos\theta_{m,n}, \cos\phi_{m,n}\cos\theta_{m,n}, 0]^{\mathrm{T}} \\ \mathbf{G}_4^{13} = \mathrm{diag}\{2d_{1,n}\nabla_\theta\mathbf{u}_{1,n}^{\mathrm{T}}\mathbf{t}_1, 2d_{2,n}\nabla_\theta\mathbf{u}_{2,n}^{\mathrm{T}}\mathbf{t}_2, \\ \qquad \cdots, 2d_{M,n}\nabla_\theta\mathbf{u}_{M,n}^{\mathrm{T}}\mathbf{t}_M\} \\ \nabla_\theta\mathbf{u}_{m,n} = [-\cos\phi_{m,n}\sin\theta_{m,n}, -\sin\phi_{m,n}\sin\theta_{m,n}, \\ \qquad \cos\theta_{m,n}]^{\mathrm{T}} \\ \mathbf{G}_4^{22} = \mathrm{diag}\{\nabla_\phi\mathbf{v}_{1,n}^{\mathrm{T}}\mathbf{t}_1, \nabla_\phi\mathbf{v}_{2,n}^{\mathrm{T}}\mathbf{t}_2, \ldots, \nabla_\phi\mathbf{v}_{M,n}^{\mathrm{T}}\mathbf{t}_M\} \\ \nabla_\phi\mathbf{v}_{m,n} = [\cos\phi_{m,n}, \sin\phi_{m,n}, 0]^{\mathrm{T}} \\ \mathbf{G}_4^{32} = \mathrm{diag}\{\nabla_\phi\mathbf{w}_{1,n}^{\mathrm{T}}\mathbf{t}_1, \nabla_\phi\mathbf{w}_{2,n}^{\mathrm{T}}\mathbf{t}_2, \ldots, \nabla_\phi\mathbf{w}_{M,n}^{\mathrm{T}}\mathbf{t}_M\} \\ \nabla_\phi\mathbf{w}_{m,n} = [-\sin\phi_{m,n}\sin\theta_{m,n}, \cos\phi_{m,n}\sin\theta_{m,n}, 0]^{\mathrm{T}} \\ \mathbf{G}_4^{33} = \mathrm{diag}\{\nabla_\theta\mathbf{w}_{1,n}^{\mathrm{T}}\mathbf{t}_1, \nabla_\theta\mathbf{w}_{2,n}^{\mathrm{T}}\mathbf{t}_2, \ldots, \nabla_\theta\mathbf{w}_{M,n}^{\mathrm{T}}\mathbf{t}_M\} \\ \nabla_\theta\mathbf{w}_{m,n} = [\cos\phi_{m,n}\cos\theta_{m,n}, \sin\phi_{m,n}\cos\theta_{m,n}, \sin\theta_{m,n}]^{\mathrm{T}} \end{cases} \tag{60}$$

■

APPENDIX 3

Proof of Proposition 2

According to the method of Lagrange multipliers, the objective function of CTLS problem (33) can be rewritten as

$$L(\mathbf{x}, \mathbf{n}_n, \boldsymbol{\lambda}) = \mathbf{n}_n^{\mathrm{T}}\mathbf{Q}_n^{-1}\mathbf{n}_n + \boldsymbol{\lambda}^{\mathrm{T}}(\tilde{\mathbf{A}}_n\mathbf{x} - \tilde{\mathbf{b}}_n - \mathbf{G}_n\mathbf{n}_n) \tag{61}$$

where $\boldsymbol{\lambda}$ is an undetermined coefficient. Taking the gradient of $L(\mathbf{x}, \mathbf{n}_n, \boldsymbol{\lambda})$ regarding $\mathbf{n}_n$ and letting it as a zero vector give

$$\frac{\partial L(\mathbf{x}, \mathbf{n}_n, \boldsymbol{\lambda})}{\partial \mathbf{n}_n} = 2\mathbf{Q}_n^{-1}\mathbf{n}_n - \mathbf{G}_n^{\mathrm{T}}\boldsymbol{\lambda} = \mathbf{0} \tag{62}$$

which can be readily recast as

$$\mathbf{n}_n = \frac{1}{2}\mathbf{Q}_n\mathbf{G}_n^{\mathrm{T}}\boldsymbol{\lambda}. \tag{63}$$

Substituting (63) into (32) gives

$$\tilde{\mathbf{A}}_n\mathbf{x} - \tilde{\mathbf{b}}_n = \frac{1}{2}\mathbf{G}_n\mathbf{Q}_n\mathbf{G}_n^{\mathrm{T}}\boldsymbol{\lambda}. \tag{64}$$

Thus, coefficient $\boldsymbol{\lambda}$ can be determined as

$$\boldsymbol{\lambda} = 2(\mathbf{G}_n\mathbf{Q}_n\mathbf{G}_n^{\mathrm{T}})^{-1}(\tilde{\mathbf{A}}_n\mathbf{x} - \tilde{\mathbf{b}}_n). \tag{65}$$

Substituting (65) into (63) gives

$$\mathbf{n}_n = \mathbf{Q}_n\mathbf{G}_n^{\mathrm{T}}(\mathbf{G}_n\mathbf{Q}_n\mathbf{G}_n^{\mathrm{T}})^{-1}(\tilde{\mathbf{A}}_n\mathbf{x} - \tilde{\mathbf{b}}_n). \tag{66}$$

Finally, substituting (66) into the objective function of CTLS problem (33) gives

$$\mathbf{n}_n^{\mathrm{T}}\mathbf{Q}_n^{-1}\mathbf{n}_n = (\tilde{\mathbf{A}}_n\mathbf{x} - \tilde{\mathbf{b}}_n)^{\mathrm{T}}(\mathbf{G}_n\mathbf{Q}_n\mathbf{G}_n^{\mathrm{T}})^{-1}(\tilde{\mathbf{A}}_n\mathbf{x} - \tilde{\mathbf{b}}_n). \tag{67}$$

Therefore, the CTLS problem (33) is equivalent to the unconstrained optimization problem (34) ■.

APPENDIX 4

Proof of Proposition 3

When the AOI measurements are obtained by all transmitters themselves, azimuth measurement vector $\mathbf{z}_\phi$ and elevation measurement vector $\mathbf{z}_\theta$ by all transmitters, and N BR measurement vectors $\mathbf{z}_{d,n}$ $(n = 1, 2, \ldots, N)$ by all receivers are transmitted to the centralized fusion center for target localization. Thus, the FIM of the centralized localization algorithm can be derived as

$$\begin{aligned} \mathbf{J} = &\sum_{i\in\mathcal{R}} \left(\frac{\partial \mathbf{z}_{d,i}}{\partial \mathbf{x}^{\mathrm{T}}}\right)^{\mathrm{T}} \mathbf{Q}_{d,i}^{-1} \frac{\partial \mathbf{z}_{d,i}}{\partial \mathbf{x}^{\mathrm{T}}} \\ &+ \left(\frac{\partial \mathbf{z}_\phi}{\partial \mathbf{x}^{\mathrm{T}}}\right)^{\mathrm{T}} \mathbf{Q}_\phi^{-1} \frac{\partial \mathbf{z}_\phi}{\partial \mathbf{x}^{\mathrm{T}}} + \left(\frac{\partial \mathbf{z}_\theta}{\partial \mathbf{x}^{\mathrm{T}}}\right)^{\mathrm{T}} \mathbf{Q}_\theta^{-1} \frac{\partial \mathbf{z}_\theta}{\partial \mathbf{x}^{\mathrm{T}}} \end{aligned} \tag{68}$$

where the subscript n is omitted in $\mathbf{z}_\phi$ and $\mathbf{z}_\theta$ since the measurements of azimuth ϕ and elevation θ are independent to receiver n. The FIM of the DCTLS algorithm given in (42) can be rewritten as

$$\mathbf{J}_n = \sum_{i\in\mathcal{R}_n} \left(\left(\frac{\partial \mathbf{z}_{d,i}}{\partial \mathbf{x}^{\mathrm{T}}}\right)^{\mathrm{T}} \mathbf{Q}_{d,i}^{-1} \frac{\partial \mathbf{z}_{d,i}}{\partial \mathbf{x}^{\mathrm{T}}} \right.$$

$$+\left(\frac{\partial \mathbf{z}_\phi}{\partial \mathbf{x}^{\mathrm{T}}}\right)^{\mathrm{T}} \mathbf{Q}_\phi^{-1} \frac{\partial \mathbf{z}_\phi}{\partial \mathbf{x}^{\mathrm{T}}} + \left(\frac{\partial \mathbf{z}_\theta}{\partial \mathbf{x}^{\mathrm{T}}}\right)^{\mathrm{T}} \mathbf{Q}_\theta^{-1} \frac{\partial \mathbf{z}_\theta}{\partial \mathbf{x}^{\mathrm{T}}}\Bigg). \quad (69)$$

Then, subtracting $\mathbf{J}$ by $\mathbf{J}_n$ yields

$$\mathbf{J}_n - \mathbf{J} = N_n \left(\left(\frac{\partial \mathbf{z}_\phi}{\partial \mathbf{x}^{\mathrm{T}}}\right)^{\mathrm{T}} \mathbf{Q}_\phi^{-1} \frac{\partial \mathbf{z}_\phi}{\partial \mathbf{x}^{\mathrm{T}}} + \left(\frac{\partial \mathbf{z}_\theta}{\partial \mathbf{x}^{\mathrm{T}}}\right)^{\mathrm{T}} \mathbf{Q}_\theta^{-1} \frac{\partial \mathbf{z}_\theta}{\partial \mathbf{x}^{\mathrm{T}}}\right) - \sum_{i \in \mathcal{R} \setminus \mathcal{R}_n} \left(\frac{\partial \mathbf{z}_{d,i}}{\partial \mathbf{x}^{\mathrm{T}}}\right)^{\mathrm{T}} \mathbf{Q}_{d,i}^{-1} \frac{\partial \mathbf{z}_{d,i}}{\partial \mathbf{x}^{\mathrm{T}}}. \quad (70)$$

Generally, the D-optimality measure, i.e., the determinant of the FIM, can be used to evaluate the localization performance [48]. The determinant of the FIM of receiver n is given by $\det(\mathbf{J}_n)$, and a larger $\det(\mathbf{J}_n)$ means that a better localization performance can be obtained. Denote $\Delta\mathbf{J}_n = \mathbf{J}_n - \mathbf{J}$. When $\Delta\mathbf{J}_n$ is a positive definite matrix, one can have

$$\det(\mathbf{J}_n + \Delta\mathbf{J}_n) > \det(\mathbf{J}_n). \quad (71)$$

That is, when condition (46) is satisfied, the proposed DCTLS algorithm can provide better localization performance than the centralized algorithm.

When the AOI measurements are obtained by all transmitters and receivers cooperatively, the AOI measurements of all receivers are independent. The FIM of the centralized localization algorithm can be derived as

$$\mathbf{J} = \sum_{i \in \mathcal{R}} \Bigg(\left(\frac{\partial \mathbf{z}_{d,i}}{\partial \mathbf{x}^{\mathrm{T}}}\right)^{\mathrm{T}} \mathbf{Q}_{d,i}^{-1} \frac{\partial \mathbf{z}_{d,i}}{\partial \mathbf{x}^{\mathrm{T}}} + \left(\frac{\partial \mathbf{z}_{\phi,i}}{\partial \mathbf{x}^{\mathrm{T}}}\right)^{\mathrm{T}} \mathbf{Q}_\phi^{-1} \frac{\partial \mathbf{z}_{\phi,i}}{\partial \mathbf{x}^{\mathrm{T}}} + \left(\frac{\partial \mathbf{z}_{\theta,i}}{\partial \mathbf{x}^{\mathrm{T}}}\right)^{\mathrm{T}} \mathbf{Q}_\theta^{-1} \frac{\partial \mathbf{z}_{\theta,i}}{\partial \mathbf{x}^{\mathrm{T}}}\Bigg). \quad (72)$$

The FIM of the DCTLS algorithm for receiver n can also be derived as

$$\mathbf{J}_n = \sum_{i \in \mathcal{R}_n} \Bigg(\left(\frac{\partial \mathbf{z}_{d,i}}{\partial \mathbf{x}^{\mathrm{T}}}\right)^{\mathrm{T}} \mathbf{Q}_{d,i}^{-1} \frac{\partial \mathbf{z}_{d,i}}{\partial \mathbf{x}^{\mathrm{T}}} + \left(\frac{\partial \mathbf{z}_{\phi,i}}{\partial \mathbf{x}^{\mathrm{T}}}\right)^{\mathrm{T}} \mathbf{Q}_\phi^{-1} \frac{\partial \mathbf{z}_{\phi,i}}{\partial \mathbf{x}^{\mathrm{T}}} + \left(\frac{\partial \mathbf{z}_{\theta,i}}{\partial \mathbf{x}^{\mathrm{T}}}\right)^{\mathrm{T}} \mathbf{Q}_\theta^{-1} \frac{\partial \mathbf{z}_{\theta,i}}{\partial \mathbf{x}^{\mathrm{T}}}\Bigg). \quad (73)$$

Generally, $\mathcal{R}_n \subseteq \mathcal{R}$, and thus $\mathbf{J}_n - \mathbf{J}$ is not a positive definite matrix. And $\mathbf{J}_n = \mathbf{J}$ can be obtained only when $\mathcal{R}_n = \mathcal{R}$. That is, the DCTLS algorithm provides the same performance as the centralized method only when the network architecture with complete connectivity for all receivers is considered. ■

REFERENCES

[1] A. M. Haimovich, R. S. Blum, and L. J. Cimini, "MIMO radar with widely separated antennas," *IEEE Signal Process. Mag.*, vol. 25, no. 1, pp. 116–129, Jan. 2008.

[2] J. Li and P. Stoica, "MIMO radar with colocated antennas," *IEEE Signal Process. Mag.*, vol. 24, no. 5, pp. 106–114, Sep. 2007.

[3] H. Godrich, A. M. Haimovich, and R. S. Blum, "Target localization accuracy gain in MIMO radar-based systems," *IEEE Trans. Inf. Theory*, vol. 56, no. 6, pp. 2783–2803, Jun. 2010.

[4] R. Niu, R. S. Blum, P. K. Varshney, and A. L. Drozd, "Target localization and tracking in noncoherent multiple-input multiple-output radar systems," *IEEE Trans. Aerosp. Electron. Syst.*, vol. 48, no. 2, pp. 1466–1489, Apr. 2012.

[5] S. Gogineni and A. Nehorai, "Target estimation using sparse modeling for distributed MIMO radar," *IEEE Trans. Signal Process.*, vol. 59, no. 11, pp. 5315–5325, Nov. 2011.

[6] W. Yi, T. Zhou, Y. Ai, and R. S. Blum, "Suboptimal low complexity joint multi-target detection and localization for non-coherent MIMO radar with widely separated antennas," *IEEE Trans. Signal Process.*, vol. 68, pp. 901–916, 2020.

[7] C.-H. Park and J.-H. Chang, "Closed-form localization for distributed MIMO radar systems using time delay measurements," *IEEE Trans. Wireless Commun.*, vol. 15, no. 2, pp. 1480–1490, Feb. 2016.

[8] A. Noroozi, M. A. Sebt, S. M. Hosseini, R. Amiri, and M. M. Nayebi, "Closed-form solution for elliptic localization in distributed MIMO radar systems with minimum number of sensors," *IEEE Trans. Aerosp. Electron. Syst.*, vol. 56, no. 4, pp. 3123–3133, Aug. 2020.

[9] R. Amiri, F. Behnia, and A. Noroozi, "Efficient joint moving target and antenna localization in distributed MIMO radars," *IEEE Trans. Wireless Commun.*, vol. 18, no. 9, pp. 4425–4435, Sep. 2019.

[10] S. A. R. Kazemi, R. Amiri, and F. Behnia, "An approximate ML estimator for moving target localization in distributed MIMO radars," *IEEE Signal Process. Lett.*, vol. 27, pp. 1595–1599, 2020.

[11] A. Noroozi, R. Amiri, M. M. Nayebi, and A. Farina, "Efficient closed-form solution for moving target localization in MIMO radars with minimum number of antennas," *IEEE Trans. Signal Process.*, vol. 68, pp. 2545–2557, 2020.

[12] Y. Du and P. Wei, "An explicit solution for target localization in noncoherent distributed MIMO radar systems," *IEEE Signal Process. Lett.*, vol. 21, no. 9, pp. 1093–1097, Sep. 2014.

[13] J. Liang, C. S. Leung, and H. C. So, "Lagrange programming neural network approach for target localization in distributed MIMO radar," *IEEE Trans. Signal Process.*, vol. 64, no. 6, pp. 1574–1585, Mar. 2016.

[14] J. Liang, Y. Chen, H.-C. So, and Y. Jing, "Circular/hyperbolic/elliptic localization via Euclidean norm elimination," *Signal Process.*, vol. 148, pp. 102–113, Feb. 2018.

[15] M. Dianat, M. R. Taban, J. Dianat, and V. Sedighi, "Target localization using least squares estimation for MIMO radars with widely separated antennas," *IEEE Trans. Aerosp. Electron. Syst.*, vol. 49, no. 4, pp. 2730–2741, Oct. 2013.

[16] M. Einemo and H. C. So, "Weighted least squares algorithm for target localization in distributed MIMO radar," *Signal Process.*, vol. 115, pp. 144–150, Oct. 2015.

[17] R. Amiri and F. Behnia, "An efficient weighted least squares estimator for elliptic localization in distributed MIMO radars," *IEEE Signal Process. Lett.*, vol. 24, no. 6, pp. 902–906, Jun. 2017.

[18] R. Amiri, F. Behnia, and H. Zamani, "Asymptotically efficient target localization from bistatic range measurements in distributed MIMO radars," *IEEE Signal. Process. Lett.*, vol. 24, no. 3, pp. 299–303, Mar. 2017.

[19] A. Noroozi and M. A. Sebt, "Target localization in multistatic passive radar using SVD approach for eliminating the nuisance parameters," *IEEE Trans. Aerosp. Electron. Syst.*, vol. 53, no. 4, pp. 1660–1671, Aug. 2017.

[20] A. Noroozi and M. A. Sebt, "Target localization from bistatic range measurements in multi-transmitter multi-receiver passive radar," *IEEE Signal. Process. Lett.*, vol. 22, no. 12, pp. 2445–2449, Dec. 2015.

[21] A. Noroozi and M. A. Sebt, "Weighted least squares target location estimation in multi-transmitter multi-receiver passive radar using bistatic range measurements," *IET Radar, Sonar Navigation*, vol. 10, no. 6, pp. 1088–1097, Jul. 2016.

[22] A. Noroozi, A. H. Oveis, and M. A. Sebt, "Iterative target localization in distributed MIMO radar from bistatic range measurements," *IEEE Signal Process. Lett.*, vol. 24, no. 11, pp. 1709–1713, Nov. 2017.

[23] H. Yang and J. Chun, "An improved algebraic solution for moving target localization in noncoherent MIMO radar systems," *IEEE Trans. Signal Process.*, vol. 64, no. 1, pp. 258–270, Jan. 2016.

[24] R. Amiri, F. Behnia, and M. A. M. Sadr, "Positioning in MIMO radars based on constrained least squares estimation," *IEEE Commun. Lett.*, vol. 21, no. 10, pp. 2222–2225, Oct. 2017.

[25] R. Amiri, F. Behnia, and M. A. M. Sadr, "Efficient positioning in MIMO radars with widely separated antennas," *IEEE Commun. Lett.*, vol. 21, no. 7, pp. 1569–1572, Jul. 2017.

[26] A. Noroozi, M. A. Sebt, and A. H. Oveis, "Efficient weighted least squares estimator for moving target localization in distributed MIMO radar with location uncertainties," *IEEE Syst. J.*, vol. 13, no. 4, pp. 4454–4463, Dec. 2019.

[27] H. Song, G. Wen, L. Zhu, and D. Li, "A novel TSWLS method for moving target localization in distributed MIMO radar systems," *IEEE Commun. Lett.*, vol. 23, no. 12, pp. 2210–2214, Dec. 2019.

[28] R. Amiri, H. Zamani, F. Behnia, and F. Marvasti, "Sparsity-aware target localization using TDOA/AOA measurements in distributed MIMO radars," *ICT Exp.*, vol. 2, no. 1, pp. 23–27, Feb. 2016.

[29] R. Amiri, F. Behnia, and H. Zamani, "Efficient 3-D positioning using time-delay and AOA measurements in MIMO radar systems," *IEEE Commun. Lett.*, vol. 21, no. 12, pp. 2614–2617, Dec. 2017.

[30] A. Noroozi and M. A. Sebt, "Algebraic solution for three-dimensional TDOA/AOA localisation in multiple-input-multiple-output passive radar," *IET Radar Sonar Navigat.*, vol. 12, no. 1, pp. 21–29, Sep. 2017.

[31] S. A. R. Kazemi, R. Amiri, and F. Behnia, "Efficient convex solution for 3-D localization in MIMO radars using delay and angle measurements," *IEEE Commun. Lett.*, vol. 23, no. 12, pp. 2219–2223, Dec. 2019.

[32] N. H. Nguyen and K. Doğançay, "Multistatic pseudolinear target motion analysis using hybrid measurements," *Signal Process.*, vol. 130, pp. 22–36, Jun. 2016.

[33] S. A. R. Kazemi, R. Amiri, and F. Behnia, "Efficient closed-form solution for 3-D hybrid localization in multistatic radars," *IEEE Trans. Aerosp. Electron. Syst.*, vol. 57, no. 6, pp. 3886–3895, Dec. 2021.

[34] S. Safavi, U. A. Khan, S. Kar, and J. M. F. Moura, "Distributed localization: A linear theory," *Proc. IEEE*, vol. 106, no. 7, pp. 1204–1223, Jul. 2018.

[35] A. Simonetto and G. Leus, "Distributed maximum likelihood sensor network localization," *IEEE Trans. Signal Process.*, vol. 62, no. 6, pp. 1424–1437, Mar. 2014.

[36] Z. Lin, T. Han, R. Zheng, and M. Fu, "Distributed localization for 2-D sensor networks with bearing-only measurements under switching topologies," *IEEE Trans. Signal Process.*, vol. 64, no. 23, pp. 6345–6359, Dec. 2016.

[37] O. Ennasr and X. Tan, "Time-difference-of-arrival (TDOA)-based distributed target localization by a robotic network," *IEEE Trans. Control Netw. Syst.*, vol. 7, no. 3, pp. 1416–1427, Sep. 2020.

[38] X. Li, X. Luo, and S. Zhao, "Globally convergent distributed network localization using locally measured bearings," *IEEE Trans. Control Netw. Syst.*, vol. 7, no. 1, pp. 245–253, Mar. 2020.

[39] Y. Liu, Y. Wang, J. Wang, and Y. Shen, "Distributed 3D relative localization of UAVs," *IEEE Trans. Veh. Technol.*, vol. 69, no. 10, pp. 11756–11770, Oct. 2020.

[40] M. A. Richards, *Fundamentals of Radar Signal Processing*. New York, NY, USA: McGraw-Hill, 2005.

[41] F. Yan, M. Jin, and X. Qiao, "Low-complexity DOA estimation based on compressed MUSIC and its performance analysis," *IEEE Trans. Signal Process.*, vol. 61, no. 8, pp. 1915–1930, Apr. 2013.

[42] S. M. Kay, *Fundamentals of Statistical Signal Processing*. Englewood Cliffs, NJ, USA: Prentice-Hall, 1993.

[43] X.-D. Zhang, *Matrix Analysis and Applications*. Cambridge, U.K.: Cambridge Univ. Press, 2017.

[44] I. Markovsky and S. Van Huffel, "Overview of total least-squares methods," *Signal Process.*, vol. 87, no. 10, pp. 2283–2302, Apr. 2007.

[45] S. A. R. Kazemi, R. Amiri, and F. Behnia, "Data association for multitarget elliptic localization in distributed MIMO radars," *IEEE Commun. Lett.*, vol. 25, no. 9, pp. 2904–2907, Sep. 2021.

[46] H. L. Van Trees and K. L. Bell, *Bayesian Bounds for Parameter Estimation and Nonlinear Filtering/Tracking*. New York, NY, USA: Wiley-Interscience, 2007.

[47] M. Xie, W. Yi, T. Kirubajaran, and L. Kong, "Joint node selection and power allocation strategy for multitarget tracking in decentralized radar networks," *IEEE Trans. Signal Process.*, vol. 66, no. 3, pp. 729–743, Feb. 2018.

[48] C. Yang, L. Kaplan, and E. Blasch, "Performance measures of covariance and information matrices in resource management for target state estimation," *IEEE Trans. Aerosp. Electron. Syst.*, vol. 48, no. 3, pp. 2594–2613, Jul. 2012.